Published in final edited form as:
Virology. 2013 September ; 444(0): 124–139. doi:10.1016/j.virol.2013.05.042.

BST-2/tetherin is overexpressed in mammary gland and tumor tissues in MMTV-induced mammary cancer

Philip H. Jones[1], **Wadie D. Mahauad-Fernandez**[1,2], **M. Nia Madison**[1], and **Chioma M. Okeoma**[1,2,*]

[1]Department of Microbiology, Carver College of Medicine, University of Iowa, Iowa City, IA, USA

[2]Interdisciplinary Graduate program in Molecular and Cellular Biology (MCB), University of Iowa, Iowa City, IA, USA

Abstract

BST-2 restricts MMTV replication, but once infection has established, MMTV modulates BST-2 levels. MMTV-directed BST-2 modulation is tissue-specific and dependent on infection and neoplastic transformation status of cells. In the lymphoid compartment of infected mice, BST-2 expression is first upregulated and then significantly downregulated regardless of absence or presence of mammary tumors. However, in mammary gland tissues, upregulation of BST-2 expression is dependent on the presence of mammary tumors and tumor tissues themselves have high BST-2 levels. Elevated BST-2 expression in these tissues is not attributable to IFN since levels of IFNα and IFNγ negatively correlate with BST-2. Importantly, soluble factors released by tumor cells suppress IFNα and IFNγ but induce BST-2. These data suggest that overexpression of BST-2 in carcinoma tissues could not be attributed to IFNs but to a yet to be determined factor that upregulates BST-2 once oncogenesis is initiated.

Keywords

BST-2; tumor; cancer; epithelial cells; mammary gland; transformation; tetherin; human breast cancer; mouse mammary tumor virus; PI3K; AKT; MIP1α; CCL3

Introduction

Breast cancer is one of the leading causes of cancer associated deaths in women. Breast cancer related deaths are in part due to complications associated with metastasis that develops in regional lymph nodes and in distant organs, including bone, lung, liver, and brain (Fisher et al., 1983). The study of breast cancer biology and pathogenesis has greatly benefited from the use of mouse models with the inherent advantage of controlled experimentation. One of the leading breast cancer models is the mouse mammary tumor

*Corresponding author: Chioma M. Okeoma, Department of Microbiology, Carver College of Medicine, University of Iowa, 51 Newton Road, Iowa City, IA 52242-1109, Office Phone: 319-335-7906, Lab Phone: 319-335-7612, Fax: 319-335-9006, chioma-okeoma@uiowa.edu.

Competing Interests: The authors have no conflicting financial interests.

Authors' contributions: CMO conceptualized and designed research, PHJ, WDM, NMN, and CMO performed research and analyzed data; CMO wrote the paper. All authors reviewed the manuscript and approved the final version.

virus (MMTV) long terminal repeat (LTR)-driven models that permit controlled neoplastic transformation of mammary glands and eventual development of mammary cancer through targeted expression of various oncogenes or by infection with MMTV. MMTV is an endemic betaretrovirus that causes mammary carcinomas upon activation (Callahan and Smith, 2000; Nusse, 1991). Several mouse strains carry MMTV and transmit the virus via the germline or through the milk of infected females. MMTV initially infects antigen presenting cells (APCs), including dendritic cells and B cells followed by T cells (Courreges et al., 2007; Ross, 2010). MMTV-mediated neoplastic transformation of mammary glands and development of mammary cancer follows after APCs and T cells have been infected by MMTV and trafficked to mammary gland, infecting mammary epithelial cells (Ross, 2010). Induction of mammary tumors by MMTV is mediated by proviral integration into the host mammary epithelial cells and activation of protooncogenes, such as Wnt genes, Fgf family genes, Notch family genes, IntH/Int5, Int6, and Int41 (Callahan and Smith, 2000; Durgam and Tekmal, 1994; Garcia et al., 1986; Gray et al., 1986; Marchetti et al., 1995), and about 33 common insertion sites recently identified in a high-throughput MMTV insertional mutagenesis screen (Szabo et al., 2005).

Integration of MMTV into the host genome could result in overexpression of natural cellular proteins or genes that are otherwise tightly regulated. Like other cancers, breast cancer results from repression, loss of function, or overexpression of one or multiple genes. One of the genes whose expression accelerates mammary tumorigenesis induced by MMTV is Akt/PKB (Young et al., 2008). Akt is a multifaceted Serine/Threonin protein kinase involved in inhibition of apoptosis and the stimulation of cellular growth. There are 3 isoforms of Akt - named Akt1, Akt2, and Akt3 that are similar in their activation/ phorsphorylation (Datta et al., 1999). Expression of different isoforms of Akt has been demonstrated in different human cancers, such as Akt1 expression in gastric and mammary cancers (Ju et al., 2007; Maroulakou et al., 2007; Staal et al., 1977; Young et al., 2008), Akt2 expression in ovarian and pancreatic cancers (Bellacosa et al., 1995; Cheng et al., 1996), and Akt3 in mammary and prostate cancer cell lines (Nakatani et al., 1999). The activation of Akt depends on activation of its upstream kinases, including Phosphatidylinositol 3-kinase (PI3K) (Datta et al., 1999). PI3K play important role in mediating cellular responses to extracellular signals (including cell survival, growth and migration) and are implicated in the progression of inflammatory diseases and cancer (Denley et al., 2008; Fougerat et al., 2009). There are three distinct sub-groups of PI3Ks namely class I (A and B), class II and class III and the classification is based on their substrate specificity and sequence homology (Vanhaesebroeck et al., 2001). The class I PI3Ks consist of four catalytic isoforms, p110α, p110β and p110δ (class IA), and p110γ (class IB); each of which is bound to a regulatory subunit (p85α, p85β, p55γ, p55α, p50α for class IA; p101 or p84 for class IB) (Krugmann et al., 1999; Stephens et al., 1997; Suire et al., 2005; Voigt et al., 2006). The different PI3K isoforms interact with distinct subsets of downstream effectors thus allowing isoform specific roles including enhancement of transcription of a diverse group of genes (Talapatra and Thompson, 2001).

It has been shown that human cells expressing MMTV sequences have enhanced transcriptional profile of proinflammatory genes, such as tumor necrosis factor (TNF), transforming growth factor beta (TGF-β), and interferon-related genes with increased

potential for cell growth (Fernandez-Cobo et al., 2006). Indeed, the transmembrane interferon-inducible gene called bone marrow stromal antigen 2 (BST-2) or tetherin and known for blocking the release of nascent enveloped viruses from the surface of infected cells (Chu et al., 2012; Dafa-Berger et al., 2012; Hammonds et al., 2012; Jones et al., 2013; Jones et al., 2012a; Kong et al., 2012; Laplana et al., 2013; Mangeat et al., 2012; Pillai et al., 2012), and inhibiting the replication of some retroviruses (Barrett et al., 2012; Jones et al., 2012a; Liberatore and Bieniasz, 2011) is overexpressed in different cancers. High levels of BST-2 were reported in multiple myelomas (Hundemer et al., 2006; Walter-Yohrling et al., 2003), metastatic ovarian cancers (Walter-Yohrling et al., 2003), neoplastic B cells (Goto et al., 1994), metastatic mammary cancers (Cai et al., 2009), and other cancer cells (Wainwright et al., 2011; Walter-Yohrling et al., 2003). Although these studies showed that BST-2 is overexpressed in cancer cells, there is no report on the progressive changes in BST-2 levels that occur in different tissues of an intact host during carcinogenesis. Here, we used C3H/HeN mouse strain to describe tissue-specific differences in the expression patterns of BST-2 in uninfected mice compared to mice suffering from MMTV infection and MMTV-induced carcinogenesis.

Results

Intrinsic expression of BST-2 in host cells potently impairs virus replication

Previously, we utilized BST-2 targeting siRNA to locally suppress BST-2 expression in murine lymph nodes and showed that down-regulation of BST-2 results in higher MMTV replication (Jones et al., 2012a). Since siRNA-dependent gene suppression is transient, we now use mice with different copies of the BST-2 gene (Fig. 1A) including homozygote WT (BST-2+/+; two copies of BST-2), homozygote knockout (BST-2−/−; no copy of BST-2), and the heterozygote (BST-2+/−; one copy of BST-2) to probe the role of BST-2 in MMTV replication. Phenotypic examination of BST-2 transcript in naïve mice shows that, as expected, BST-2−/− mice have no BST-2 mRNA in the lymph node and spleen (Fig. 1B). However, mice with one copy of the BST-2 gene (BST-2+/−) express about half BST-2 mRNA compared to the WT mice (Fig. 1B). Similarly, BST-2 surface protein was higher in WT mice compared to their BST-2+/− counterpart (Fig. 1C). Since BST-2 mRNA is not present in BST-2−/− mice, we did not examine the surface protein. *Ex vivo* infection of lymphocytes and splenocytes obtained from WT, BST-2+/−, and BST-2−/− mice show that BST-2−/− mice have significantly higher MMTV proviral sequences as detected by real-time PCR amplification of the viral genome (Fig. 1D). Subcutaneous inoculation of MMTV into murine footpad tissues show that *in vivo*, MMTV replicates much better in BST-2−/− mice compared to BST-2+/−, and WT in that order (Fig. 1E). The spread of infection was also higher in BST-2−/− mice since more proviral sequence is detected in the spleen of BST-2−/− mice than BST-2+/− and WT mice (Fig. 1F). These data support our initial finding (Jones et al., 2012a) and reveal that loss of BST-2 predisposes mice to significant MMTV replication. Because expression of BST-2 significantly reduces viral load, we examined the impact of acute MMTV infection on BST-2 expression. Thus, we queried the level of BST-2 surface protein and mRNA in the lymph nodes and spleens of MMTV infected WT and BST-2+/− mice using FACS and RT-qPCR respectively. We observed a substantial increase in BST-2 surface protein (Figs. 1G and 1H) and mRNA (Figs. 1I and 1J)

day 1 post infection. This increase was followed by a significant decrease 7 days later (Figs. 1G to 1J). To determine whether higher viral products are released by infected BST-2−/− mice, we quantified plasma viral loads by measuring the level of cell-free plasma reverse transcriptase (RT) activity between WT, BST-2+/−, and BST-2−/− mice day 1 and 7 after infection. Virion-associated RT activity as determined by Molecular Probes EnzCheck Reverse Transcriptase assay was significantly higher in BST-2−/− mice compared to BST-2+/−, and WT mice in that order (Fig.1K).

Milk-borne infection of mice with MMTV results in changes in BST-2 expression

To further understand the effect of MMTV on BST-2 expression, we examined the levels of BST-2 expression in mice infected via the natural route. Spleens from age-matched pups nursed on C3H/HeN•MMTV− (naïve) and C3H/HeN•MMTV+ (infected) mice were examined for BST-2 expression using FACS analysis (Figs. 2A and 2B) and RT-qPCR (Fig. 2C). We observed that in the naïve mice, level of BST-2 protein and mRNA were lowest at day 3 and thereafter a steady increase up to day 30 (Figs. 2A and 2C). In contrast, BST-2 surface protein and mRNA levels were highest in milk-borne infected mice at day 3 with a significant decline on days 7, 21, and 30 (Figs. 2B and 2C). Examination of the proviral sequence by PCR reveals that naïve mice lack MMTV sequence as expected while infected mice harbor the proviral sequence (Fig. 2D). Of note, levels of proviral DNA were lower on day 3 compared to others days. This difference in the levels of proviral DNA could be attributed to the age of the animals. Furthermore, since level of BST-2 expression in MMTV infected mice decrease with age, we examined the level of BST-2 in age-matched naïve and milk-borne infected adult (5 weeks old) female mice. Results show that similar to the weanlings, levels of BST-2 protein and mRNA in infected mice are significantly lower compared to the level in their naïve counterparts (Figs. 2A to 2C). The suppression in BST-2 expression was observed with respect to BST-2 transcript (Fig. 2E) and surface protein (Fig. 2F) in peripheral blood mononuclear cells (PBMCs), spleens, and lymph nodes. As expected, the infected mice harbor MMTV proviral sequence in their chromosomes (Fig. 2G).

Induction of mammary cancer by MMTV results in tissue specific changes in BST-2 and viral nucleic acids expression in the lymphoid compartment

The major pathology observed in MMTV infected mice is mammary cancer. Different inbred strains of mice have different incidences and types of cancers. Some strains such as C57BL are resistant to MMTV-induced mammary cancer while others such as C3H and BALB/c are very susceptible to mammary cancer development. The C3H strain has a high incidence (>70%) of mammary cancer development in both virgin and breeding mice, while C57BL has a very low incidence (<5%). Given the high propensity of MMTV-induced mammary cancer in C3H/HeN and the fact that no significant difference exist in BST-2 mRNA expression between C57BL/6 and C3H/HeN mice (Jones et al., 2012a), we used C3H/HeN•MMTV+ non-tumor bearing (infected) and C3H/HeN•MMTV+ tumor-bearing (tumor-bearing) mice to further dissect the effect of MMTV on BST-2 expression in mice infected with MMTV and suffering from mammary cancer. Comparison of BST-2 expression levels in the lymphoid compartments (PBMCs, spleen, and lymph node) that are targets of MMTV infection using RT-qPCR and FACS show levels of BST-2 mRNA (Fig.

3A) and protein (Fig. 3B) to be significantly lower in PBMCs, spleen, and lymph nodes of tumor-bearing mice. Levels of cell associated proviral DNA (VDNA) and viral RNA (VRNA) were higher in these tissues (Figs. 3C and 3D). The thymus, another target of MMTV, had significantly lower BST-2 in non-tumor bearing mice as shown for other lymphoid organs (Fig. 3E). However, the thymi of tumor-bearing mice have 5 times more BST-2 mRNA compared to the levels in the naïve thymi (Fig. 3E) and the level of cell associated VDNA (Fig. 3F) and VRNA (Fig. 3G) in the thymi of tumor-bearing mice was also higher compared to that in non-tumor bearing mice.

Changes in BST-2 and viral nucleic acid levels in non-lymphoid tissues

Although MMTV does not replicate well in non-lymphoid tissues, expression of MMTV proviral DNA was demonstrated in C3Hf/HeSed mouse liver, kidney, lung, and intestine (Chen et al., 1990). Moreover, presence of MMTV-like envelope sequences has been shown in liver biopsies of disease but not in normal human liver (Johal et al., 2009). To determine the impact of MMTV on BST-2 levels in non-lymphoid tissues, we used RT-qPCR to evaluate level of BST-2 mRNA and viral nucleic acids in bone marrow cells, liver, lung, heart, and kidney. Our data show that as in the lymphoid tissues, BST-2 levels is significantly lower in bone marrow cells, lung, liver, and heart of MMTV infected and tumor-bearing mice compared to the naïve mice (Figures 4A to 4D). But in the kidney, MMTV did not change the level of BST-2 in infected mice and there was a slight but non-significant increase in BST-2 mRNA in the kidney of tumor-bearing mice (Figure 4E). In contrast to level of BST-2, both viral RNA and proviral DNA expression are significantly higher in liver, lung, heart, and kidney, but not in bone marrow cells of tumor-bearing mice compared to infected mice (Figures 4F to 4I). Although BST-2 expression is suppressed in lung, liver, and heart of infected and tumor-bearing mice to similar levels, viral nucleic acids level differed, with the tumor-bearing mice harboring significantly more viral products, especially notable in the heart (Figures 4H and 4I).

BST-2 is highly overexpressed in tumor tissues and mammary glands of tumor-bearing mice

Since MMTV infects mammary gland cells resulting neoplastic epithelial cell transformation, we examined the levels of BST-2 in mammary gland tissues of naïve mice, non-tumor-bearing mice and tumor-bearing mice. RT-qPCR data reveal that while no significant change occurred in BST-2 mRNA levels of naïve and infected non tumor-bearing mice, expression of BST-2 transcript was about 8 times higher in the mammary gland tissues of tumor bearing mice (Fig. 5A). Comparison of BST-2 levels in mammary gland and tumor tissues show that BST-2 level is significantly higher in tumor tissues compared to mammary gland tissues obtained from the same tumor-bearing mice (Fig. 5B). We also used FACS analysis to compare the levels of BST-2 surface protein in lymphoid and tumor tissues from the same animal and show that BST-2 surface protein is significantly higher in tumor tissues (Fig. 5C).

Increased BST-2 expression in mammary gland and mammary tumor tissues from tumor-bearing mice correlates with high tissue and plasma viral load

BST-2 functions to block the replication of MMTV following experimental infection of mice (Figs. 1D to 1G). Moreover, lower levels of BST-2 mRNA and surface protein observed in lymphoid and non-lymphoid tissues of tumor-bearing mice (Figs. 3A, 3B, 4B to 4D) inversely correlates with level of viral nucleic acids in these lymphoid cells (Figs. 3C and 3D) with the thymi as an exception (Figs. 3E to 3G). In the thymus, BST-2 mRNA was slightly suppressed in MMTV infected mice but upregulated in the thymi from tumor-bearing mice (Fig. 3E). Although BST-2 mRNA is significantly higher in the thymi of tumor-bearing mice compared to their non-tumor bearing counterparts, both VDNA and VRNA levels were also higher in the tumor-bearing mice (Figs. 3F and 3G), suggesting that high level of BST-2 may be responsible for accumulation of viral nucleic acids or that BST-2 is not restricting virus replication in the thymi. To determine whether high BST-2 levels in mammary gland and tumor tissues correlate with viral gene expression, we subjected DNA and RNA samples from these tissues to qPCR and RT-qPCR respectively. We show that in spite of the high BST-2 mRNA in mammary glands from tumor-bearing mice, these tissues contain significantly more VDNA (Fig. 5D) and VRNA (Fig. 5E) when compared to mammary glands from infected non tumor-bearing mice. Comparison between mammary gland and tumor tissues from the same tumor-bearing mice indicates that tumor tissues harbor more viral DNA and RNA than mammary gland tissues (Figs. 5F and 5G); again despite high BST-2 level (Figs. 5B). To assess level of cell-free virus in these mice, we measured RT activity in cell-free plasma. Figure 5I show that tumor-bearing mice harbor about 14 times more cell-free virus in their plasma compared to their non-tumor bearing counterparts (Fig. 5I). Together, these data suggest that high levels of BST-2 in mammary gland and tumor tissues do not impact cell associated and cell-free viral load in mice suffering from MMTV-induced mammary cancer.

BST-2 is overexpressed in mammary carcinoma epithelial cells

Although both mammary gland and mammary tumor tissues consist of many different cell types, including fibroblasts, adipocytes, inflammatory cells and epithelial cells, mammary carcinomas are epithelial neoplasms. Hence, we examined levels of BST-2 mRNA and surface protein in normal murine mammary epithelial cells (NMuMG) and mammary carcinoma cells (Mm5MT and 4T1). We observed that both 4T1 and Mm5MT cells have comparable levels of BST-2 mRNA (Fig. 6A) and surface protein (Fig. 6B). BST-2 levels in these carcinoma cell lines are significantly higher than that in normal mammary epithelia (Fig.6A and 6B). Since Mm5MT cells were derived from mammary tumor of C3H/HeN mice, we wondered if BST-2 levels in the tumor and tumor-derived epithelial cells will be comparable. RT-qPCR analysis showed that although mammary carcinoma cells express more BST-2 compared to normal mammary epithelia control, FACS and RT-qPCR analysis reveal that significant differences exist among tumor tissues, mammary gland from tumor-bearing mice, tumor-derived mammary gland cells, and normal mammary gland cells (Fig. 6C). Compared to normal mammary epithelial cells, BST-2 levels are higher in mammary carcinoma epithelial cells, mammary gland tissues, and tumor tissues in that order. To determine whether higher BST-2 expression impacts viral load, we examined the level of cell associated viral nucleic acids (DNA and RNA). We observed significantly higher viral

gene expression in the form of integrated provirus and viral RNA (Fig. 6D), as well as viral protein (Fig. 6E) in mammary gland and tumor tissues in that order; compared to Mm5MT cells.

High levels of BST-2 in tumor-derived mammary epithelial cells, mammary gland, and mammary tumor tissues correlate with levels of PI3K, MIP-1α/CCL3, and AKT mRNAs

Since Integration of MMTV into the host genome could change expression patterns of multiple genes, we sought to identify other genes whose expressions correlate with BST-2. High levels of phosphoinositide 3 kinase (PI3K) have been reported in different cancers (Fransson et al., 2013), making PI3K a good candidate gene. Examination of PI3K expression show that the genes encoding the different isoforms (PI3KCA, PI3KCB, PI3KCD, PI3KCG) of the catalytic subunit of PI3K are highly elevated in mammary gland tissues (Fig. 7A). PI3KCA was approximately 100 times and 250 times higher in mammary gland tissues from infected and tumor-bearing mice respectively compared to their naïve counterpart (Fig. 7A). Comparison of mRNA levels of PI3K isoform subunits between mammary gland and tumor tissues revealed a slight increase in PI3KCA and PI3KCB in tumor tissues over mammary gland (Fig. 7B). The high levels of the catalytic PI3K isoforms led us to evaluate the level of the regulatory subunit of PI3K (encoded by PIK3R1). Our analysis reveals that no differences exist in PI3KR1 levels in mammary gland and tumor tissues (Fig. 7C). Furthermore, significant induction of PI3KCA, PI3KCB, PI3KCD, and PI3KCG was observed in Mm5MT cells over NMuMG cells (Fig. 7D). However, PI3KR1 level was not significantly different between Mm5MT and NMuMG cells (Fig. 7E). Because AKT is the effector of PI3K and AKT expression has been shown to influence MMTV-induce mammary tumorigenesis (Young et al., 2008), we examined the level of AKT expression in mammary gland and tumor tissues. Our data reveal that AKT1 and AKT3 isoforms are elevated in infected mammary gland tissue but AKT2 is downregulated (Fig. 8A). Similarly, levels of AKT1 and AKT3 are also elevated in mammary gland of tumor-bearing mice over tumor tissue and non-tumor bearing mammary gland tissues in that order (Fig. 8B). Moreover, AKT1 and AKT3 but not AKT2 are elevated in Mm5MT cells compared to NMuMG cells (Fig. 8C). This result prompted us to examine the expression levels of the two forms of phospho-Akt (pAktS^{473} and pAKTT^{308}). Both naïve and MMTV infected mammary gland tissues express pAktS^{473} and pAKTT^{308} (Fig. 8D). Examination of pAkt levels in infected non-tumor-bearing mammary gland, tumor-bearing mammary gland and tumor tissues show no change in pAkt expression (Fig. 8E).

Given that the PI3K pathway is activated by macrophage inflammatory protein 1-alpha (MIP1-α/CCL3) (Lentzsch et al., 2003) and MIP1-α/CCL3 plays important role in amplifying inflammation (Staudt et al., 2013), we examined the level of MIP1-α/CCL3 in mammary and tumor tissues. As was observed for BST-2 and PI3K, MIP1-α/CCL3 mRNA level is highly elevated in mammary gland and tumor tissues compared to naïve mammary gland (Fig. 8F). Moreover, MIP1-α/CCL3 mRNA level in Mm5MT cells is also elevated compared to the level in NMuMGs (Fig. 8G). These data show positive correlative expression levels of BST-2, PI3K, AKT, and MIP1-α/CCL3 in tumor-derived mammary epithelial cells, mammary gland, and tumor tissues, and indicate that BST-2 is not the only elevated gene during MMTV-induced carcinogenesis.

Level of IFNα inversely correlates with BST-2 in tumor-bearing mice

It is well known that BST-2 expression is principally induced by IFNs (Jones et al., 2013; Jones et al., 2012a; Yoo et al., 2011). To assess the level of types I and II IFN during MMTV pathogenesis and to determine whether levels of IFNs correlate with BST-2, we evaluated the transcripts of IFNα and IFNγ in representative lymphoid, mammary, and tumor tissues from naïve, infected, and tumor-bearing mice. In the lymphoid compartment (lymph node and PBMC), IFNα was repressed in both infected and tumor-bearing mice but IFNγ was induced in infected mice (Figs. 9A and 9B). In contrast, both IFNα and IFNγ mRNA were significantly suppressed in the mammary gland tissues of infected and tumor-bearing mice (Fig. 9C). There was no significant difference in levels of IFNα and IFNγ between mammary gland and tumor tissues, although level of IFNα was slightly lower in tumor tissues (Fig. 9D). We also compared expression levels of IFNα and IFNγ in normal and tumor-derived mammary epithelial cells and showed that as with tissues from tumor-bearing mice, tumor-derived mammary epithelial cells have significantly lower levels of both IFNα and IFNγ transcripts compared to normal mammary epithelial cells (Fig. 9E). IFN protein levels were not assessed since level of IFNα mRNA was low in all tissues tested and there is no correlation between BST-2 and IFNs mRNA. Our data indicate that mice suffering from MMTV-induced mammary cancer have suppressed levels of IFNα and IFNγ expression, suggesting that these IFNs may not be responsible for inducing BST-2 in mammary gland and tumor tissues.

Media conditioned by primary mammary tumor cells block types I and II IFNs and elevate BST-2 expression in normal mammary epithelial cells *ex vivo*

Since BST-2 expression is enhanced but IFNα and IFNγ expression are impaired in mammary and tumor tissues, we wanted to evaluate the impact of soluble factors secreted by tumor cells on BST-2 and IFNs expression. We used an in vitro culture model to mimic the *in vivo* microenvironment by exposing normal mammary epithelial cells (NMuMGs) to supernatants derived from single cell suspension of primary tumor cells (tumor conditioned medium, TCM). We also exposed normal mammary epithelial cells to supernatants derived from single cell suspensions of splenocytes exposed to LPS (splenocyte conditioned medium, SCM) for positive control. We observed that while normal mammary epithelial BST-2 protein (Fig. 9A) and mRNA (Fig. 9B) were highly induced by tumor-conditioned medium (TCM), IFNα and IFNβ mRNA (Fig. 9C) were significantly suppressed by TCM. In contrast, SCM significantly mediated the induction of BST-2, IFNα, and IFNγ expression (Figs. 9A to 9C). These data suggest that soluble factors secreted by tumor cells may be partly responsible for inducing BST-2 expression in mammary epithelial cells. Moreover, our data is in agreement with a published report which showed that breast tumor environment blocks type IFN production (Sisirak et al., 2013). To identify the soluble factors present in TCM, we used mouse inflammatory cytokines multi-analyte ELISArray Kit to identify the cytokines secreted into culture medium. Results show increased levels of interleukin 6 (IL6) and Granulocyte colony-stimulating factor (G-CSF) in TCM compared to medium alone (Fig. 9D). Studies are ongoing to determine whether these factors are directly involved in mediating BST-2 induction.

Discussion

Overexpression of BST-2 gene has been detected in various human tumor cell lines and tissues (Cai et al., 2009; Hundemer et al., 2006; Wainwright et al., 2011; Walter-Yohrling et al., 2003), and an earlier study showed that neoplastic B cells have high level of BST-2 (Goto et al., 1994). Here, we show that BST-2 is overexpressed in mammary gland and tumor tissues from MMTV tumor-bearing mice, as well as in mammary carcinoma cell lines isolated from MMTV-induced mammary cancer. MMTV is a useful tool for identifying genes that play a role in viral pathogenesis and human mammary tumorigenesis. It has been suggested that the incidence of human breast cancer correlates with risk factors such as age, diet, obesity, family history (Kelsey, 1993; Szabo et al., 2005), and distribution of MMTV in house mice (Stewart et al., 2000). Although knowledge about the involvement of MMTV in human mammary carcinogenesis is still evolving, MMTV is thought to be involved in human mammary carcinogenesis due to the identification of sequences homologous to the env gene of MMTV in about 40% of human breast cancers (Faedo et al., 2004; Ford et al., 2004; Langerod et al., 2007; Wang et al., 2003). Hence, understanding the role of BST-2 in MMTV infection and MMTV-induced mammary carcinogenesis could improve our understanding of the biology and pathogenesis of mammary cancer.

In this study, we used mice with different genetic makeup to examine the effect of BST-2 expression in infection of MMTV target tissues and analyzed the impact of MMTV infection on the expression levels of BST-2. We found that expression of BST-2 in target tissues/cells blocks the replication of MMTV. Endogenous RT assay revealed that viral load was significantly higher in BST-2−/− mice compared to their BST-2+/− and WT counterparts. Higher RT activity in BST-2−/− plasma may indicate that more virions are released by infected BST-2−/− mice or it could be a marker of higher viral load since it has been suggested that endogenous RT activity is the best surrogate measure of infectious HIV-1 titer (Liu et al., 2010). Although BST-2 inhibits MMTV replication, we found that MMTV modulates BST-2 expression in a biphasic manner. MMTV first enhances BST-2 expression both during footpad inoculation and gut infection via contaminated breast milk. The increase in BST-2 levels is followed by significant down modulation days later. In the lymphoid compartments which are targets of MMTV infection (Ross, 2010), BST-2 expression was high 24 hours after infection followed by a significant decline. This observation is partly in line with an earlier demonstration that BST-2 expression is significantly high during acute HIV infection of PBMCs (Homann et al., 2011). Similar to the observation in lymphoid tissues, BST-2 levels in non-lymphoid tissues, including bone marrow, liver, lung, and heart, but not kidney was suppressed by infection with MMTV. Indeed, viruses such as HIV and chikungunya virus use different mechanisms, including removal of BST-2 from the cell membrane and BST-2 degradation to regulate BST-2 expression and neutralize its anti-viral activity (Goffinet et al., 2010; Jones et al., 2012a; Neil et al., 2008; Perez-Caballero et al., 2009; Radoshitzky et al., 2010; Skasko et al., 2012; Watanabe et al., 2011). It is therefore possible that MMTV modulates BST-2 levels to allow its replication.

Since MMTV is an oncoRNAvirus (Allred and Medina, 2008; Callahan and Smith, 2008; Dickson et al., 1984; Kim et al., 2011; Kuriki et al., 2000; Marcotte and Muller, 2008) and infection with this virus results in oncogenic transformation of mammary gland tissues and

tumor induction, we hypothesized that modulation of BST-2 in mammary gland tissues will depend on transformation status of the mammary epithelia, with transformed epithelial cells expressing lower levels of BST-2 similar to the lymphoid tissues. Remarkably, we observed tissue specific differences in BST-2 expression in mice during the course of MMTV infection. Compared to naïve mice, BST-2 levels in lymphoid, non-lymphoid, and mammary tissue compartments in MMTV infected non-tumor bearing mice was significantly lower. Furthermore, in comparison to their infected non tumor-bearing counterparts or uninfected (naïve) controls, mice bearing mammary tumors have significantly high BST-2 mRNA and surface protein levels in the mammary gland and tumor tissues. However, in their lymphoid and non-lymphoid tissues with the exception of the thymus and kidney, BST-2 is significantly repressed. The observed tissue specificity in BST-2 expression prompted us to examine the level of viral genetic materials in the respective tissues to determine whether higher BST-2 expression will inversely correlate with viral loads, in agreement with the role of BST-2 in restricting acute infection (Homann et al., 2011; Jones et al., 2012a). Unexpectedly, BST-2 levels in the thymus, mammary gland and tumor tissues positively correlate with proviral DNA and viral RNA levels in these tissues. In contrast, we observed negative correlation between BST-2 level and viral nucleic acids in liver, lung, heart, and kidney of tumor-bearing mice. These observations partly agrees and partly contradicts the anti-viral function of BST-2 as clearly demonstrated in figure 1, which shows that loss of BST-2 gene enhances cell-associated viral nucleic acids expression and cell-free virion associated RT activity. It therefore seems that once infection establishes and mammary cell transformation initiates, BST-2 may lose its anti-viral potency or in addition to its anti-viral function, may assume a role in tumorigenesis that is yet to be determined.

Because mammary carcinomas are epithelial neoplasms, we used different mammary carcinoma epithelial cell lines to probe the regulation of BST-2 by MMTV. Compared to normal mammary epithelial cells, BST-2 mRNA and surface protein levels are significantly higher in the transformed epithelial cells although not to the level observed in mammary gland and tumor tissues. The differences in BST-2 expression may stem from the fact that the epithelial cells are homogenous while mammary gland and mammary tumor tissues consist of many different cell types such as macrophages that may have different expression profiles than the epithelial cells. Nonetheless, BST-2 expression is about 6 times higher in carcinoma mammary epithelial cells than in normal mammary epithelia. Interestingly, examination of known tumor stimulatory factors, including PI3K, AKT, and MIP1α/CCL3 reveals elevated levels of all 3 genes in carcinoma cells and tissues compared to normal cells/tissues. PI3K, AKT, and MIP1α/CCL3 have been implicated in a variety of normal and patho-physiological responses, involving regulation of immune response and pathogenesis of different cancers, such as has been reported for the involvement of Akt1 in murine mammary cancer (Maroulakou et al., 2007; Young et al., 2008) and elevated levels of MIP1α/CCL3 in human breast cancer (Burger et al., 2009), or promotion of angiogenesis by MIP1α/CCL3 (Wu et al., 2008). The finding that expression patterns of BST-2, PI3K, AKT, and MIP1α/CCL3 are altered in mammary tissues during MMTV infection and MMTV-induced mammary carcinogenesis may imply that elevated BST-2 levels may be an epiphenomenon of proviral expression and tumor growth. It could also be that BST-2 plays a critical role in mammary tumorigenesis. Indeed, published reports have implicated BST-2 as

a tumor promoting gene as shown with the demonstration that the application of anti-BST2 antibody to endometrial cancer cells resulted in cytotoxic effect in BST2-positive cells (Yokoyama et al., 2012). Similarly, anti-BST-2 antibody substantially reduced tumor growth in mice (Schliemann et al., 2010). In contrast, there is evidence that BST-2 could function as an inhibitor of cancer cell growth and migration since BST-2 inhibits membrane type 1-matrix metalloproteinase (MT1-MMP)-mediated cell growth and migration (Gu et al., 2012).

Many factors have been implicated in upregulation of BST-2 expression, notably IFNα (Jones et al., 2013; Jones et al., 2012a), IFNγ (Yoo et al., 2011), and even viral infections (Homann et al., 2011). However, we found that chronic infection with MMTV suppresses both BST-2 and IFNα and upon tumor development, both IFNα and IFNγ are suppressed, while BST-2 is elevated. While changes in BST-2 during mammary cancer has not been reported prior to our study, our data on IFNα suppression is in agreement with published data which demonstrated suppressed levels of type I IFNs (α/β) and TNFα (Sisirak et al., 2013) in mammary cancer. Thus, induction of BST-2 in tumor-derived mammary epithelial cells, mammary gland, and tumor tissues could not be attributed to IFNα and IFNγ since very low expression of these IFNs were observed in tissues from tumor bearing mice. Although it is known that BST-2 is an IFNα-regulated gene, it has been reported that engagement of Ig-like Transcript 7 (ILT7) by BST2 regulates plasmacytoid dendritic cell-mediated production of IFNα (Cao et al., 2009). Therefore in tumor cells, it may be possible that shut down of IFNα production is facilitated by BST-2. However, this does not explain the low level of IFNα in tissues with low BST-2 levels such as some lymphoid and non-lymphoid tissues.

In the absence of IFNs expression, increased BST-2 expression observed in carcinoma tissues could be attributed to tumor cells themselves, peritumoral cells present at the tumor site, or to soluble factors released by tumor cells. In our studies, we found that tumor conditioned medium (TCM) induced BST-2 surface protein and mRNA but suppressed IFNα and IFNγ mRNA in normal mammary epithelial cells. It is well known that cancer cell-derived soluble factors mediate different biological activities (Guerrero et al., 2010; Li and Galileo, 2010; Toulza et al., 2005) and that soluble factors released by breast tumor block type I IFN production (Sisirak et al., 2013). Our study identified IL6 and G-CSF as soluble factors present in high levels in TCM. Although a recent study found that IL6 does not induce BST2, it is noteworthy that the referenced study was conducted on human monocytes and T cells (Guzzo et al., 2012). That being said, we have not directly tested whether recombinant IL6 or G-CSF could induce BST-2 in mammary epithelial and/or tumor cells. It is however interesting that we observed the presence of both IL6 and G-CSF in TCM because previous work by others have shown that IL6 and G-CSF are produced by tumor and/or stromal cells in malignant tumors (Shojaei et al., 2007). IL6 and G-CSF in conjunction with phospho-STAT3 have been implicated in the protumor function of neutrophils (Yan et al., 2013). Furthermore, G-CSF is involved in promoting tumor angiogenesis (Okazaki et al., 2006; Shojaei et al., 2009) and increased levels of serum IL-6 have been associated with poor prognosis in human mammary cancer (Zhang and Adachi, 1999).

While the role of BST-2 in mammary tumorigenesis is yet to be determined, we speculate that misregulated gene expression commonly observed during mammary cell transformation and/or soluble factors in tumor microenvironment may be at least partly responsible for BST-2 upregulation. Upon induction, BST-2 may serve as an adhesion molecule by preferentially recruiting various cell types from blood to the site of inflammation and/or facilitating tumor cell contact with the endothelium, thus, contributing to cancer metastasis and progression. Consistent with this idea is the finding that the monocytic cell line U937 adheres to BST-2 extracellular domain-coated tissue culture wells (Yoo et al., 2011). Further studies are therefore required to identify other cellular sources of BST-2 in mammary gland and mammary tumor tissues, as well as decipher the role of BST-2 in mammary carcinogenesis.

Experimental Procedures

Ethics statement

All experiments involving mice were performed in accordance to NIH guidelines, the Animal Welfare Act, and US federal law. The experiments were approved by the University of Iowa Animal Care and Use Committee (IACUC). Mice were housed according to the policies of the Institutional Animal Care and Use Committee of the University of Iowa.

Animals

BST-2−/− mice generated with 129/SvJ mice (Swiecki et al., 2012) were kindly provided by Dr. Marco Colonna of Washington University, MO. BST-2−/− females were backcrossed to C57BL/6 males for 9 generations. WT and BST-2+/− mice were generated from crosses between BST-2−/− and WT and PCR genotyped where applicable. C3H/HeN•MMTV+ and C3H/HeN•MMTV− were purchased from the National Cancer Institute (NCI). C3H/HeN•MMTV+ were bred for 2 pregnancies after which the males were removed to prevent future pregnancy and slow time to tumor development or the mice were force-bred until mammary tumor developed. Mice were sacrificed in accordance to the policies of the University of Iowa Institutional Animal Care and Use Committee.

Infection of mice

In vivo infection of mice was performed as previously described (Jones et al., 2012b; Mehta et al., 2012; Okeoma et al., 2010; Okeoma et al., 2007; Okeoma et al., 2009a; Okeoma et al., 2009b; Okeoma et al., 2008). At different times after infection, mice were sacrificed and relevant tissues were harvested. Tissues and/or single cells derived from tissues were used for downstream analysis.

Cell lines

NMuMG (derived from normal mammary tissue of a Namru mouse strain) and Mm5MT (a mouse mammary carcinoma cell line from C3H/HeN mouse strain) were purchased from American Type Culture Collection (ATCC). 4T1 (a mouse mammary carcinoma cell line from Balb/c mouse strain) is a kind gift from Dr. Lyse Norian of the University of Iowa. All cells were maintained according to the suppliers' instructions.

Generation of primary tumor cells

Mammary tumors were aseptically excised from the mammary fatpad of C3H/HeN•MMTV + mice into PBS. Tumor explants were washed with PBS first and then homogenized in serum-free RPMI-1640. Tumor homogenates were digested in RPMI-1640 containing 0.2% Collagenase A, 5% FBS, 0.2% Trypsin, and 5ug/ml Gentamycin at 37°C for 30 minutes with shaking at 100 rpm. Tumor digest were passed through a cell strainer and cells pelleted. Cells were cultured in RPMI-1640 containing 10%FBS, and 1% penicillin/streptomycin.

Conditioned medium

Tumor cell conditioned medium (TCM) obtained from primary tumor cells and splenocyte conditioned medium (SCM) obtained from LPS-treated splenocytes were prepared as follows. Single cells from tumor cells or splenocytes were plated in 3-wells of 6-well plate. LPS at 1μg/ml was added to the splenocyte culture and allowed to incubate for 15 minutes. Splenocytes were washed and resuspended in fresh medium. All cells were allowed to incubate at 37°C for 24 hours. Prior to treatment of epithelial cells, conditioned TCM and SCM were collected, centrifuged for 10 minutes at 2000 rpm and then filtered through a 0.22-μm filter (VWR). The media were placed on ice and UV-treated for 1 hour followed by ultracentrifugation for 3 hours at 32000 rpm. Supernatants were used to treat cells.

Antibodies

Goat anti-p27 (capsid) has been previously described (Jones et al., 2012a; Okeoma et al., 2007; Okeoma et al., 2008). Anti-pAKT^{S473}, anti-pAKT^{T308}, and anti-AKT were purchased from Cell Signaling Technology. Alexa flour 647 conjugated anti-mouse BST-2 clone 129c, and FITC conjugated anti-mouse BST-2 clone 927 purchased from eBioscience. Goat anti-GAPDH was from Santa Cruz Biotech and IRDye 800CW donkey anti-goat was purchased from Li-core.

Western blots

Western blots were performed as previously described (Jones et al., 2012b; Mehta et al., 2012; Okeoma et al., 2009a). Blots were probed with anti-p27, anti-pAKT^{S473}, anti-pAKT^{T308}, anti-AKT, and anti-GAPDH depending on experiment. The species-appropriate IRDye secondary antibodies were used followed by detection with the Odyssey Infrared Imaging System (LI-COR Biosciences).

ELISA

Cytokine/Chemokine Multi-Analyte ELISA Array (Qiagen, USA) was performed according to manufacturer's instructions. Briefly, cell culture supernatant samples were centrifuged at 1000×g for 10 minutes to remove particulate material. Assay buffer (50 μl) was added to each well of the ELISA plate followed by 50 μl of sample or antigen standard cocktail. The plate was then covered, gently swirled for 10 seconds and incubated at room temperature for 2 hours. The contents of the wells were decanted and wells were washed three times with 350 μl of wash buffer. Detection antibody diluted in assay buffer (100 μl) was added to the wells, gently swirled and incubated for 1 hour at room temperature. The plate was washed three times. Avidin-HRP diluted in assay buffer (100 μl) was added to the wells, gently

swirled and incubated in the dark for 30 minutes at room temperature. The plate was washed four times. Development solution (100 μl) was added to the wells and incubated in the dark for 15 minutes. Stop solution (100 μl) was added to the wells and the absorbance was read at 450 nm using a Tecan Infinite M200 PRO plate reader (Tecan).

DNA, RNA isolation and real-time quantitative PCR (qPCR)

Isolation of DNA and RNA were accomplished using ZR-Duet DNA/RNA MiniPrep (ZYMO Research) according to manufacturer's instructions. For cDNA synthesis, equivalent amounts of RNA treated with DNase I (Qiagen) were reverse-transcribed with high capacity cDNA reverse transcription Kit (ABI), and the cDNA was amplified with target specific primers. Semi-quantitative PCR was performed using ABI Veriti 96-Well thermal cycler; quantitative real time qPCR (qPCR) and reverse transcription real time qPCR (RT-qPCR) were carried out using ABI 7500 FAST thermal cycler. Sequences of primer pairs used are available upon request.

Flow cytometry

Approximately, 1×10^6 Mm5MT, NMuMG, 4T1, and lymphocytes were stained in PBS with relevant antibodies as previously described (Jones et al., 2012a; Okeoma et al., 2008). Following extensive washes, cells were fixed with 2% paraformaldehyde and subjected to FACS. Using FACS calibur flow cytometer (BD), at least ten-thousand events were collected for each sample. FACS data were analyzed by Flowjo software (TreeStar).

Reverse transcriptase assay

Reverse transcriptase activity was determined in cell-free plasma according to the manufacturer's recommended protocol (Molecular Probes EnzCheck Reverse Transcriptase Assay Kit). Briefly, 5 μl of poly (A) ribonucleotide template was added to 5 μl of oligo d (T) 16 primer and incubated at room temperature for 1 hour. Template/primer solution was diluted 200 fold in polymerization buffer and 20 μl aliquots were added to wells of a black optical bottom plate (Thermo Fisher). Samples and standards (GeneMate room temperature 200 U/μl) were diluted 2 fold in 50 mM Tris-HCL, 20% glycerol, 2 mM DTT, pH 7.6. 5 μl of samples or standards were added to the reaction mixture in the wells of the black optical bottom plate and incubated at room temperature for 1 hour. The reaction was stopped with 2 μl of 200 mM EDTA per sample/standard. 173 μl of PicoGreen working solution diluted in TE buffer was added to the samples/standards and incubated at room temperature for 5 minutes. Fluorescence (Ex: 480 nm, Em: 520 nm) was measured using a fluorescent plate reader (Tecan Infinate M200 PRO, Tecan Austria/Europe). Reverse transcriptase activity of the samples was calculated from the reverse transcriptase standard curve.

Statistical analysis

Statistical analysis of significant differences was tested using paired two-tailed Student's t test. A p value of 0.05 was considered significant. Error bars represent standard deviations.

Acknowledgments

We are very grateful to Drs. Marco Colonna of Washington University and Lyse Norian of the University of Iowa for providing the BST-2−/− mice and 4T1 cells respectively. Our appreciation goes to Bryson Okeoma for important editorial input. This research was supported by University of Iowa Startup funds to CMO. PHJ was supported by immunology T32 training grant to the University of Iowa. MNM was supported by Infectious Diseases T32 training grant to the University of Iowa. WDM was partly supported by University of Iowa MCB program.

List of abbreviations

BST-2	bone marrow stromal cell antigen 2
NMuMG	normal murine mammary gland
FACS	Fluorescence activated cell sorting
PI3K	Phosphoinositide 3 kinase
MIP1-α	Macrophage inflammatory protein 1-alpha

References

Allred DC, Medina D. The relevance of mouse models to understanding the development and progression of human breast cancer. Journal of mammary gland biology and neoplasia. 2008; 13:279–288. [PubMed: 18704660]

Barrett BS, Smith DS, Li SX, Guo K, Hasenkrug KJ, Santiago ML. A single nucleotide polymorphism in tetherin promotes retrovirus restriction in vivo. PLoS Pathog. 2012; 8:e1002596. [PubMed: 22457621]

Bellacosa A, de Feo D, Godwin AK, Bell DW, Cheng JQ, Altomare DA, Wan M, Dubeau L, Scambia G, Masciullo V, Ferrandina G, Benedetti Panici P, Mancuso S, Neri G, Testa JR. Molecular alterations of the AKT2 oncogene in ovarian and breast carcinomas. International journal of cancer. Journal international du cancer. 1995; 64:280–285. [PubMed: 7657393]

Burger JA, Quiroga MP, Hartmann E, Burkle A, Wierda WG, Keating MJ, Rosenwald A. High-level expression of the T-cell chemokines CCL3 and CCL4 by chronic lymphocytic leukemia B cells in nurselike cell cocultures and after BCR stimulation. Blood. 2009; 113:3050–3058. [PubMed: 19074730]

Cai D, Cao J, Li Z, Zheng X, Yao Y, Li W, Yuan Z. Up-regulation of bone marrow stromal protein 2 (BST2) in breast cancer with bone metastasis. BMC cancer. 2009; 9:102. [PubMed: 19338666]

Callahan R, Smith GH. MMTV-induced mammary tumorigenesis: gene discovery, progression to malignancy and cellular pathways. Oncogene. 2000; 19:992–1001. [PubMed: 10713682]

Callahan R, Smith GH. Common integration sites for MMTV in viral induced mouse mammary tumors. Journal of mammary gland biology and neoplasia. 2008; 13:309–321. [PubMed: 18709449]

Cao W, Bover L, Cho M, Wen X, Hanabuchi S, Bao M, Rosen DB, Wang YH, Shaw JL, Du Q, Li C, Arai N, Yao Z, Lanier LL, Liu YJ. Regulation of TLR7/9 responses in plasmacytoid dendritic cells by BST2 and ILT7 receptor interaction. The Journal of experimental medicine. 2009; 206:1603–1614. [PubMed: 19564354]

Chen RF, Good RA, Engelman RW, Hamada N, Tanaka A, Nonoyama M, Day NK. Suppression of mouse mammary tumor proviral DNA and protooncogene expression: association with nutritional regulation of mammary tumor development. Proceedings of the National Academy of Sciences of the United States of America. 1990; 87:2385–2389. [PubMed: 2157199]

Cheng JQ, Ruggeri B, Klein WM, Sonoda G, Altomare DA, Watson DK, Testa JR. Amplification of AKT2 in human pancreatic cells and inhibition of AKT2 expression and tumorigenicity by antisense RNA. Proceedings of the National Academy of Sciences of the United States of America. 1996; 93:3636–3641. [PubMed: 8622988]

Chu H, Wang JJ, Qi M, Yoon JJ, Chen X, Wen X, Hammonds J, Ding L, Spearman P. Tetherin/BST-2 is essential for the formation of the intracellular virus-containing compartment in HIV-infected macrophages. Cell host & microbe. 2012; 12:360–372. [PubMed: 22980332]

Courreges MC, Burzyn D, Nepomnaschy I, Piazzon I, Ross SR. Critical role of dendritic cells in mouse mammary tumor virus in vivo infection. Journal of virology. 2007; 81:3769–3777. [PubMed: 17267484]

Dafa-Berger A, Kuzmina A, Fassler M, Yitzhak-Asraf H, Shemer-Avni Y, Taube R. Modulation of hepatitis C virus release by the interferon-induced protein BST-2/tetherin. Virology. 2012; 428:98–111. [PubMed: 22520941]

Datta SR, Brunet A, Greenberg ME. Cellular survival: a play in three Akts. Genes & development. 1999; 13:2905–2927. [PubMed: 10579998]

Denley A, Gymnopoulos M, Hart JR, Jiang H, Zhao L, Vogt PK. Biochemical and biological characterization of tumor-associated mutations of p110alpha. Methods in enzymology. 2008; 438:291–305. [PubMed: 18413256]

Dickson C, Smith R, Brookes S, Peters G. Tumorigenesis by mouse mammary tumor virus: proviral activation of a cellular gene in the common integration region int-2. Cell. 1984; 37:529–536. [PubMed: 6327073]

Durgam VR, Tekmal RR. The nature and expression of int-5, a novel MMTV integration locus gene in carcinogen-induced mammary tumors. Cancer letters. 1994; 87:179–186. [PubMed: 7812938]

Faedo M, Ford CE, Mehta R, Blazek K, Rawlinson WD. Mouse mammary tumor-like virus is associated with p53 nuclear accumulation and progesterone receptor positivity but not estrogen positivity in human female breast cancer. Clinical cancer research : an official journal of the American Association for Cancer Research. 2004; 10:4417–4419. [PubMed: 15240531]

Fernandez-Cobo M, Melana SM, Holland JF, Pogo BG. Transcription profile of a human breast cancer cell line expressing MMTV-like sequences. Infectious agents and cancer. 2006; 1:7. [PubMed: 17173685]

Fisher B, Bauer M, Wickerham DL, Redmond CK, Fisher ER, Cruz AB, Foster R, Gardner B, Lerner H, Margolese R, et al. Relation of number of positive axillary nodes to the prognosis of patients with primary breast cancer. An NSABP update. Cancer. 1983; 52:1551–1557. [PubMed: 6352003]

Ford CE, Faedo M, Crouch R, Lawson JS, Rawlinson WD. Progression from normal breast pathology to breast cancer is associated with increasing prevalence of mouse mammary tumor virus-like sequences in men and women. Cancer research. 2004; 64:4755–4759. [PubMed: 15256443]

Fougerat A, Gayral S, Malet N, Briand-Mesange F, Breton-Douillon M, Laffargue M. Phosphoinositide 3-kinases and their role in inflammation: potential clinical targets in atherosclerosis? Clinical science (London, England 1979). 2009; 116:791–804.

Fransson S, Abel F, Kogner P, Martinsson T, Ejeskar K. Stage-dependent expression of PI3K/Aktpathway genes in neuroblastoma. International journal of oncology. 2013; 42:609–616. [PubMed: 23232578]

Garcia M, Wellinger R, Vessaz A, Diggelmann H. A new site of integration for mouse mammary tumor virus proviral DNA common to BALB/cf(C3H) mammary and kidney adenocarcinomas. The EMBO journal. 1986; 5:127–134. [PubMed: 3007110]

Goffinet C, Homann S, Ambiel I, Tibroni N, Rupp D, Keppler OT, Fackler OT. Antagonism of CD317 restriction of human immunodeficiency virus type 1 (HIV-1) particle release and depletion of CD317 are separable activities of HIV-1 Vpu. J Virol. 2010; 84:4089–4094. [PubMed: 20147395]

Goto T, Kennel SJ, Abe M, Takishita M, Kosaka M, Solomon A, Saito S. A novel membrane antigen selectively expressed on terminally differentiated human B cells. Blood. 1994; 84:1922–1930. [PubMed: 8080996]

Gray DA, McGrath CM, Jones RF, Morris VL. A common mouse mammary tumor virus integration site in chemically induced precancerous mammary hyperplasias. Virology. 1986; 148:360–368. [PubMed: 3002039]

Gu G, Zhao D, Yin Z, Liu P. BST-2 binding with cellular MT1-MMP blocks cell growth and migration via decreasing MMP2 activity. Journal of cellular biochemistry. 2012; 113:1013–1021. [PubMed: 22065321]

Guerrero J, Tobar N, Caceres M, Espinoza L, Escobar P, Dotor J, Smith PC, Martinez J. Soluble factors derived from tumor mammary cell lines induce a stromal mammary adipose reversion in human and mice adipose cells. Possible role of TGF-beta1 and TNF-alpha. Breast cancer research and treatment. 2010; 119:497–508. [PubMed: 19649705]

Guzzo C, Jung M, Graveline A, Banfield BW, Gee K. IL-27 increases BST-2 expression in human monocytes and T cells independently of type I IFN. Scientific reports. 2012; 2:974. [PubMed: 23240078]

Hammonds J, Wang JJ, Spearman P. Restriction of Retroviral Replication by Tetherin/BST-2. Molecular biology international. 2012; 2012:424768. [PubMed: 22811908]

Homann S, Smith D, Little S, Richman D, Guatelli J. Upregulation of BST-2/Tetherin by HIV infection in vivo. Journal of virology. 2011; 85:10659–10668. [PubMed: 21849457]

Hundemer M, Schmidt S, Condomines M, Lupu A, Hose D, Moos M, Cremer F, Kleist C, Terness P, Belle S, Ho AD, Goldschmidt H, Klein B, Christensen O. Identification of a new HLA-A2-restricted T-cell epitope within HM1.24 as immunotherapy target for multiple myeloma. Experimental hematology. 2006; 34:486–496. [PubMed: 16569595]

Johal H, Scott GM, Jones R, Camaris C, Riordan S, Rawlinson WD. Mouse mammary tumour virus-like virus (MMTV-LV) is present within the liver in a wide range of hepatic disorders and unrelated to nuclear p53 expression or hepatocarcinogenesis. Journal of hepatology. 2009; 50:548–554. [PubMed: 19168254]

Jones PH, Maric M, Madison MN, Maury W, Roller RJ, Okeoma CM. BST-2/tetherin-mediated restriction of chikungunya (CHIKV) VLP budding is counteracted by CHIKV non-structural protein 1 (nsP1). Virology. 2013; 438:37–49. [PubMed: 23411007]

Jones PH, Mehta HV, Maric M, Roller RJ, Okeoma CM. Bone marrow stromal cell antigen 2 (BST-2) restricts mouse mammary tumor virus (MMTV) replication in vivo. Retrovirology. 2012a; 9:10. [PubMed: 22284121]

Jones PH, Mehta HV, Okeoma CM. A novel role for APOBEC3: susceptibility to sexual transmission of murine acquired immunodeficiency virus (mAIDS) is aggravated in APOBEC3 deficient mice. Retrovirology. 2012b; 9:50. [PubMed: 22691411]

Ju X, Katiyar S, Wang C, Liu M, Jiao X, Li S, Zhou J, Turner J, Lisanti MP, Russell RG, Mueller SC, Ojeifo J, Chen WS, Hay N, Pestell RG. Akt1 governs breast cancer progression in vivo. Proceedings of the National Academy of Sciences of the United States of America. 2007; 104:7438–7443. [PubMed: 17460049]

Kelsey JL. Breast cancer epidemiology: summary and future directions. Epidemiologic reviews. 1993; 15:256–263. [PubMed: 8405209]

Kim HH, van den Heuvel AP, Schmidt JW, Ross SR. Novel common integration sites targeted by mouse mammary tumor virus insertion in mammary tumors have oncogenic activity. PloS one. 2011; 6:e27425. [PubMed: 22087314]

Kong WS, Irie T, Yoshida A, Kawabata R, Kadoi T, Sakaguchi T. Inhibition of virus-like particle release of Sendai virus and Nipah virus, but not that of mumps virus, by tetherin/CD317/BST-2. Hiroshima journal of medical sciences. 2012; 61:59–67. [PubMed: 23077864]

Krugmann S, Hawkins PT, Pryer N, Braselmann S. Characterizing the interactions between the two subunits of the p101/p110gamma phosphoinositide 3-kinase and their role in the activation of this enzyme by G beta gamma subunits. The Journal of biological chemistry. 1999; 274:17152–17158. [PubMed: 10358071]

Kuriki K, Kamiakito T, Yoshida H, Saito K, Fukayama M, Tanaka A. Integration of proviral sequences, but not at the common integration sites of the FGF8 locus, in an androgen-dependent mouse mammary Shionogi carcinoma. Cellular and molecular biology (Noisy-le-Grand, France). 2000; 46:1147–1156.

Langerod A, Zhao H, Borgan O, Nesland JM, Bukholm IR, Ikdahl T, Karesen R, Borresen-Dale AL, Jeffrey SS. TP53 mutation status and gene expression profiles are powerful prognostic markers of breast cancer. Breast cancer research : BCR. 2007; 9:R30. [PubMed: 17504517]

Laplana M, Caruz A, Pineda JA, Puig T, Fibla J. Association of BST-2 gene variants with HIV disease progression underscores the role of BST-2 in HIV type 1 infection. The Journal of infectious diseases. 2013; 207:411–419. [PubMed: 23148293]

Lentzsch S, Gries M, Janz M, Bargou R, Dorken B, Mapara MY. Macrophage inflammatory protein 1-alpha (MIP-1 alpha) triggers migration and signaling cascades mediating survival and proliferation in multiple myeloma (MM) cells. Blood. 2003; 101:3568–3573. [PubMed: 12506012]

Li Y, Galileo DS. Soluble L1CAM promotes breast cancer cell adhesion and migration in vitro, but not invasion. Cancer cell international. 2010; 10:34. [PubMed: 20840789]

Liberatore RA, Bieniasz PD. Tetherin is a key effector of the antiretroviral activity of type I interferon in vitro and in vivo. Proc Natl Acad Sci U S A. 2011; 108:18097–18101. [PubMed: 22025715]

Liu Y, Wang C, Mueller S, Paul AV, Wimmer E, Jiang P. Direct Interaction between Two Viral Proteins, the Nonstructural Protein 2CATPase and the Capsid Protein VP3, Is Required for Enterovirus Morphogenesis. PLoS pathogens. 2010; 6

Mangeat B, Cavagliotti L, Lehmann M, Gers-Huber G, Kaur I, Thomas Y, Kaiser L, Piguet V. Influenza virus partially counteracts restriction imposed by tetherin/BST-2. The Journal of biological chemistry. 2012; 287:22015–22029. [PubMed: 22493439]

Marchetti A, Buttitta F, Miyazaki S, Gallahan D, Smith GH, Callahan R. Int-6, a highly conserved, widely expressed gene, is mutated by mouse mammary tumor virus in mammary preneoplasia. Journal of virology. 1995; 69:1932–1938. [PubMed: 7853537]

Marcotte R, Muller WJ. Signal transduction in transgenic mouse models of human breast cancer--implications for human breast cancer. Journal of mammary gland biology and neoplasia. 2008; 13:323–335. [PubMed: 18651209]

Maroulakou IG, Oemler W, Naber SP, Tsichlis PN. Akt1 ablation inhibits, whereas Akt2 ablation accelerates, the development of mammary adenocarcinomas in mouse mammary tumor virus (MMTV)-ErbB2/neu and MMTV-polyoma middle T transgenic mice. Cancer research. 2007; 67:167–177. [PubMed: 17210696]

Mehta HV, Jones PH, Weiss JP, Okeoma CM. IFN-alpha and lipopolysaccharide upregulate APOBEC3 mRNA through different signaling pathways. Journal of immunology (Baltimore, Md. 1950). 2012; 189:4088–4103.

Nakatani K, Sakaue H, Thompson DA, Weigel RJ, Roth RA. Identification of a human Akt3 (protein kinase B gamma) which contains the regulatory serine phosphorylation site. Biochemical and biophysical research communications. 1999; 257:906–910. [PubMed: 10208883]

Neil SJ, Zang T, Bieniasz PD. Tetherin inhibits retrovirus release and is antagonized by HIV-1 Vpu. Nature. 2008; 451:425–430. [PubMed: 18200009]

Nusse R. Insertional mutagenesis in mouse mammary tumorigenesis. Current topics in microbiology and immunology. 1991; 171:43–65. [PubMed: 1667629]

Okazaki T, Ebihara S, Asada M, Kanda A, Sasaki H, Yamaya M. Granulocyte colony-stimulating factor promotes tumor angiogenesis via increasing circulating endothelial progenitor cells and Gr1+CD11b+ cells in cancer animal models. International immunology. 2006; 18:1–9. [PubMed: 16352631]

Okeoma CM, Huegel AL, Lingappa J, Feldman MD, Ross SR. APOBEC3 proteins expressed in mammary epithelial cells are packaged into retroviruses and can restrict transmission of milk-borne virions. Cell host & microbe. 2010; 8:534–543. [PubMed: 21147467]

Okeoma CM, Lovsin N, Peterlin BM, Ross SR. APOBEC3 inhibits mouse mammary tumour virus replication in vivo. Nature. 2007; 445:927–930. [PubMed: 17259974]

Okeoma CM, Low A, Bailis W, Fan HY, Peterlin BM, Ross SR. Induction of APOBEC3 in vivo causes increased restriction of retrovirus infection. Journal of virology. 2009a; 83:3486–3495. [PubMed: 19153238]

Okeoma CM, Petersen J, Ross SR. Expression of murine APOBEC3 alleles in different mouse strains and their effect on mouse mammary tumor virus infection. Journal of virology. 2009b; 83:3029–3038. [PubMed: 19153233]

Okeoma CM, Shen M, Ross SR. A novel block to mouse mammary tumor virus infection of lymphocytes in B10.BR mice. Journal of virology. 2008; 82:1314–1322. [PubMed: 18003725]

Perez-Caballero D, Zang T, Ebrahimi A, McNatt MW, Gregory DA, Johnson MC, Bieniasz PD. Tetherin inhibits HIV-1 release by directly tethering virions to cells. Cell. 2009; 139:499–511. [PubMed: 19879838]

Pillai SK, Abdel-Mohsen M, Guatelli J, Skasko M, Monto A, Fujimoto K, Yukl S, Greene WC, Kovari H, Rauch A, Fellay J, Battegay M, Hirschel B, Witteck A, Bernasconi E, Ledergerber B, Gunthard HF, Wong JK. Role of retroviral restriction factors in the interferon-alpha-mediated suppression of HIV-1 in vivo. Proceedings of the National Academy of Sciences of the United States of America. 2012; 109:3035–3040. [PubMed: 22315404]

Radoshitzky SR, Dong L, Chi X, Clester JC, Retterer C, Spurgers K, Kuhn JH, Sandwick S, Ruthel G, Kota K, Boltz D, Warren T, Kranzusch PJ, Whelan SP, Bavari S. Infectious Lassa virus, but not filoviruses, is restricted by BST-2/tetherin. J Virol. 2010; 84:10569–10580. [PubMed: 20686043]

Ross SR. Mouse mammary tumor virus molecular biology and oncogenesis. Viruses. 2010; 2:2000–2012. [PubMed: 21274409]

Schliemann C, Roesli C, Kamada H, Borgia B, Fugmann T, Klapper W, Neri D. In vivo biotinylation of the vasculature in B-cell lymphoma identifies BST-2 as a target for antibody-based therapy. Blood. 2010; 115:736–744. [PubMed: 19903902]

Shojaei F, Wu X, Qu X, Kowanetz M, Yu L, Tan M, Meng YG, Ferrara N. G-CSF-initiated myeloid cell mobilization and angiogenesis mediate tumor refractoriness to anti-VEGF therapy in mouse models. Proceedings of the National Academy of Sciences of the United States of America. 2009; 106:6742–6747. [PubMed: 19346489]

Shojaei F, Wu X, Zhong C, Yu L, Liang XH, Yao J, Blanchard D, Bais C, Peale FV, van Bruggen N, Ho C, Ross J, Tan M, Carano RA, Meng YG, Ferrara N. Bv8 regulates myeloid-cell-dependent tumour angiogenesis. Nature. 2007; 450:825–831. [PubMed: 18064003]

Sisirak V, Vey N, Goutagny N, Renaudineau S, Malfroy M, Thys S, Treilleux I, Labidi-Galy SI, Bachelot T, Dezutter-Dambuyant C, Menetrier-Caux C, Blay JY, Caux C, Bendriss-Vermare N. Breast cancer-derived transforming growth factor-beta and tumor necrosis factor-alpha compromise interferon-alpha production by tumor-associated plasmacytoid dendritic cells. International journal of cancer. Journal international du cancer. 2013

Skasko M, Wang Y, Tian Y, Tokarev A, Munguia J, Ruiz A, Stephens EB, Opella SJ, Guatelli J. HIV-1 Vpu protein antagonizes innate restriction factor BST-2 via lipid-embedded helix-helix interactions. The Journal of biological chemistry. 2012; 287:58–67. [PubMed: 22072710]

Staal SP, Hartley JW, Rowe WP. Isolation of transforming murine leukemia viruses from mice with a high incidence of spontaneous lymphoma. Proceedings of the National Academy of Sciences of the United States of America. 1977; 74:3065–3067. [PubMed: 197531]

Staudt ND, Jo M, Hu J, Bristow JM, Pizzo DP, Gaultier A, Vandenberg SR, Gonias SL. Myeloid cell receptor LRP1/CD91 regulates monocyte recruitment and angiogenesis in tumors. Cancer research. 2013

Stephens LR, Eguinoa A, Erdjument-Bromage H, Lui M, Cooke F, Coadwell J, Smrcka AS, Thelen M, Cadwallader K, Tempst P, Hawkins PT. The G beta gamma sensitivity of a PI3K is dependent upon a tightly associated adaptor, p101. Cell. 1997; 89:105–114. [PubMed: 9094719]

Stewart TH, Sage RD, Stewart AF, Cameron DW. Breast cancer incidence highest in the range of one species of house mouse, Mus domesticus. British journal of cancer. 2000; 82:446–451. [PubMed: 10646903]

Suire S, Coadwell J, Ferguson GJ, Davidson K, Hawkins P, Stephens L. p84, a new Gbetagamma-activated regulatory subunit of the type IB phosphoinositide 3-kinase p110gamma. Current biology : CB. 2005; 15:566–570. [PubMed: 15797027]

Swiecki M, Wang Y, Gilfillan S, Lenschow DJ, Colonna M. Cutting edge: paradoxical roles of BST2/tetherin in promoting type I IFN response and viral infection. Journal of immunology (Baltimore, Md. 1950). 2012; 188:2488–2492.

Szabo S, Haislip AM, Garry RF. Of mice, cats, and men: is human breast cancer a zoonosis? Microscopy research and technique. 2005; 68:197–208. [PubMed: 16276516]

Talapatra S, Thompson CB. Growth factor signaling in cell survival: implications for cancer treatment. The Journal of pharmacology and experimental therapeutics. 2001; 298:873–878. [PubMed: 11504779]

Toulza F, Eliaou JF, Pinet V. Breast tumor cell soluble factors induce monocytes to produce angiogenic but not angiostatic CXC chemokines. International journal of cancer. Journal international du cancer. 2005; 115:429–436. [PubMed: 15688373]

Vanhaesebroeck B, Leevers SJ, Ahmadi K, Timms J, Katso R, Driscoll PC, Woscholski R, Parker PJ, Waterfield MD. Synthesis and function of 3-phosphorylated inositol lipids. Annual review of biochemistry. 2001; 70:535–602.

Voigt P, Dorner MB, Schaefer M. Characterization of p87PIKAP, a novel regulatory subunit of phosphoinositide 3-kinase gamma that is highly expressed in heart and interacts with PDE3B. The Journal of biological chemistry. 2006; 281:9977–9986. [PubMed: 16476736]

Wainwright DA, Balyasnikova IV, Han Y, Lesniak MS. The expression of BST2 in human and experimental mouse brain tumors. Experimental and molecular pathology. 2011; 91:440–446. [PubMed: 21565182]

Walter-Yohrling J, Cao X, Callahan M, Weber W, Morgenbesser S, Madden SL, Wang C, Teicher BA. Identification of genes expressed in malignant cells that promote invasion. Cancer research. 2003; 63:8939–8947. [PubMed: 14695211]

Wang Y, Melana SM, Baker B, Bleiweiss I, Fernandez-Cobo M, Mandeli JF, Holland JF, Pogo BG. High prevalence of MMTV-like env gene sequences in gestational breast cancer. Medical oncology (Northwood, London, England). 2003; 20:233–236.

Watanabe R, Leser GP, Lamb RA. Influenza virus is not restricted by tetherin whereas influenza VLP production is restricted by tetherin. Virology. 2011; 417:50–56. [PubMed: 21621240]

Wu Y, Li YY, Matsushima K, Baba T, Mukaida N. CCL3-CCR5 axis regulates intratumoral accumulation of leukocytes and fibroblasts and promotes angiogenesis in murine lung metastasis process. Journal of immunology (Baltimore, Md. 1950). 2008; 181:6384–6393.

Yan B, Wei JJ, Yuan Y, Sun R, Li D, Luo J, Liao SJ, Zhou YH, Shu Y, Wang Q, Zhang GM, Feng ZH. IL-6 Cooperates with G-CSF To Induce Protumor Function of Neutrophils in Bone Marrow by Enhancing STAT3 Activation. Journal of immunology (Baltimore, Md. 1950). 2013; 190:5882–5893.

Yokoyama T, Enomoto T, Serada S, Morimoto A, Matsuzaki S, Ueda Y, Yoshino K, Fujita M, Kyo S, Iwahori K, Fujimoto M, Kimura T, Naka T. Plasma membrane proteomics identifies bone marrow stromal antigen 2 as a potential therapeutic target in endometrial cancer. International journal of cancer. Journal international du cancer. 2012

Yoo H, Park SH, Ye SK, Kim M. IFN-gamma-induced BST2 mediates monocyte adhesion to human endothelial cells. Cellular immunology. 2011; 267:23–29. [PubMed: 21094940]

Young CD, Nolte EC, Lewis A, Serkova NJ, Anderson SM. Activated Akt1 accelerates MMTV-c-ErbB2 mammary tumourigenesis in mice without activation of ErbB3. Breast cancer research : BCR. 2008; 10:R70. [PubMed: 18700973]

Zhang GJ, Adachi I. Serum interleukin-6 levels correlate to tumor progression and prognosis in metastatic breast carcinoma. Anticancer research. 1999; 19:1427–1432. [PubMed: 10365118]

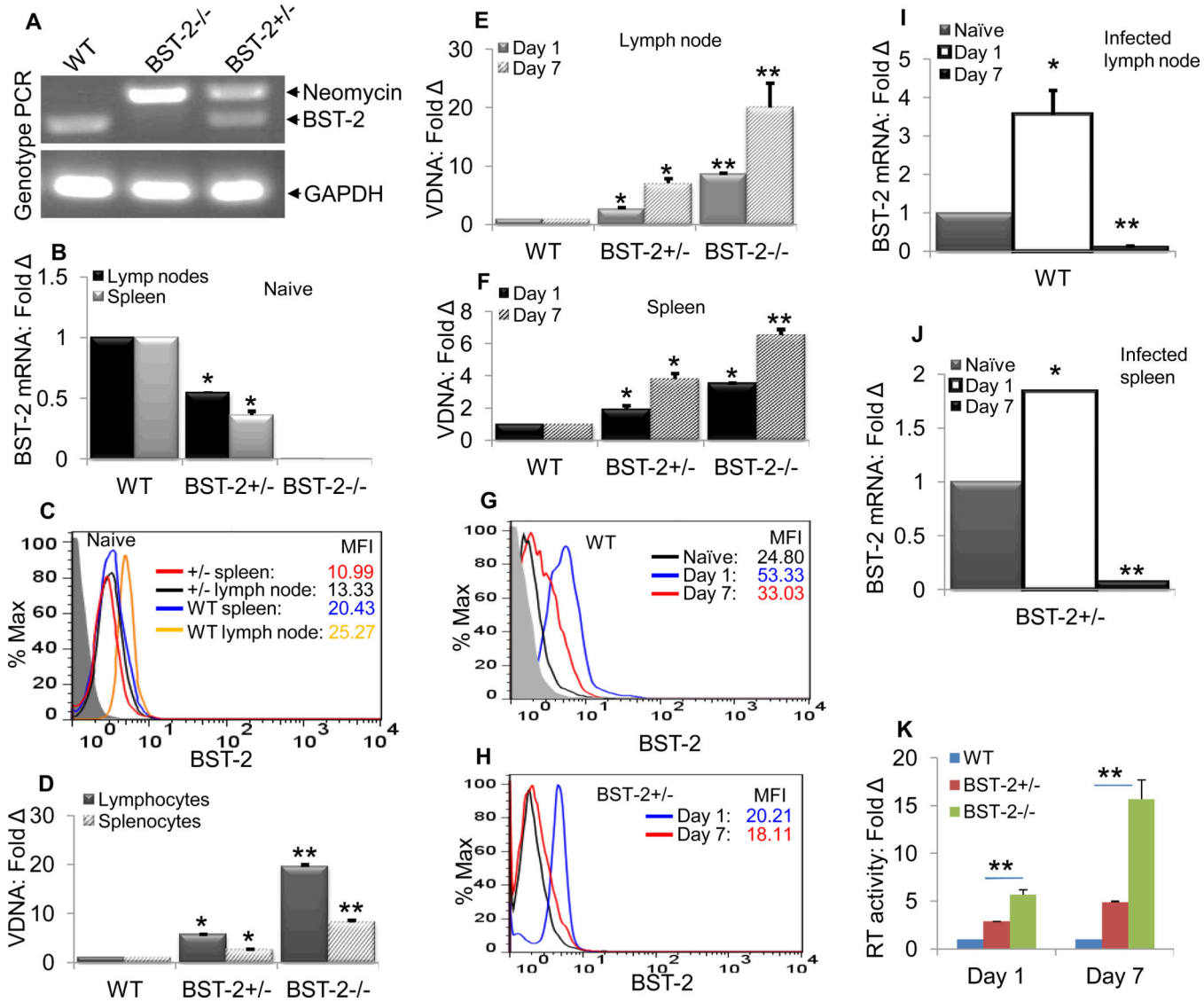

Figure 1. Restriction of MMTV replication by BST-2 present in host target cells and modulation of BST-2 by MMTV

Homozygote WT and BST-2−/− mice were crossed to generate the heterozygote BST-2+/− mice. The genotypes were confirmed by PCR with primers that detect endogenous BST-2 and neomycin following previously described protocol (Swiecki et al., 2012) (A). WT, BST-2+/− (+/−), and BST-2−/− (−/−) mice (n = 5/genotype) were phenotyped for BST-2 expression by RT-qPCR using BST-2 specific primers (B) or by FACS - fluorescence activated cell sorting (C). Lymphocytes and splenocytes obtained from WT, BST-2+/− (+/−), and BST-2−/− (−/−) mice were infected e*x vivo* with MMTV. DNA isolated from cells was examined for level of infection by qPCR 24 hours later (D). Naïve age-matched WT, BST+/−, and BST-2−/− mice (n = 5/genotype/time point) were infected with MMTV by subcutaneous injection on the hind footpad. On days 1 and 7, groups of 5 mice/genotype were sacrificed. Single cells from the lymph nodes and spleens were used for qPCR (E and F), FACS (G and H), and RT-qPCR (I and J) to determine the level of virus replication, surface level of BST-2, and BST-2 transcripts respectively. (K) RT-based plasma viral loads

as determined by Molecular Probes EnzCheck Reverse Transcriptase Assay was performed with cell-free plasma from WT, BST-2+/−, and BST-2−/− mice (n = 5) infected with MMTV for 1 and 7 days. RT activity of the samples was extrapolated from the RT standard curve and presented as fold change of RT units in 1 μl of WT plasma. PCR data are normalized to GAPDH and presented as fold change relative to proviral DNA (VDNA) or BST-2 mRNA in WT mice. Error bars are standard deviation; ** is significance with p value less than 0.01 and * is significance with p value less than 0.05. The numbers next to histogram legend denote mean florescence intensity (MFI) of surface BST-2 levels. Experiments were performed with 5 mice per genotype and repeated at least 3 times with similar results.

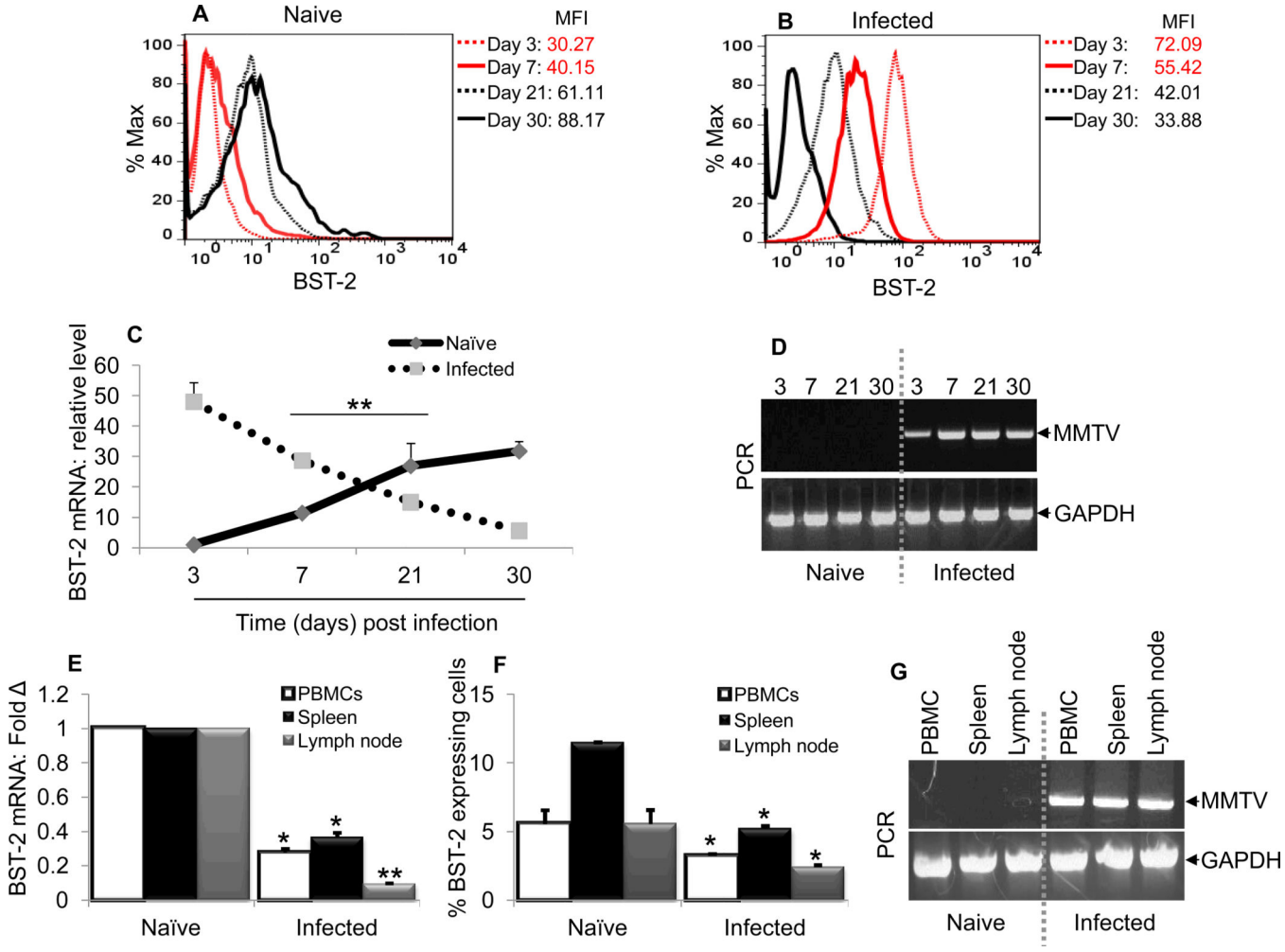

Figure 2. MMTV acquired via the natural route regulates BST-2 expression

Age-matched C3H/HeN•MMTV- and C3H/HeN•MMTV+ mice (n = 3) were bred. Their pups (n = 5/time point) were sacrificed at different time points (3, 7, 21, and 30 days) as shown on the figures. At necropsy, splenocytes were subjected to FACS analysis of BST-2 surface protein (A and B), RT-qPCR of BST-2 mRNA expression (C), and PCR of MMTV proviral DNA levels (D). PBMCs were obtained from adult (5 weeks old) C3H/HeN•MMTV− (naïve) and C3H/HeN•MMTV+ (infected) mice (n = 3) prior to sacrifice. At necropsy, spleens and lymph nodes, as well as the isolated PBMCs were subjected to RT-qPCR examination of BST-2 levels following RNA isolation and cDNA synthesis (E), FACS analysis of surface BST-2 (F). DNA isolated from the cells was used for PCR examination of proviral DNA (G). RT-PCR data are normalized to GAPDH and presented as relative levels (C) or as fold change relative to BST-2 mRNA in naïve mice (E). GAPDH was also used as loading control (D and G). Error bars are standard deviation; ** is significance with p value less than 0.01 and * is significance with p value less than 0.05. The numbers next to histogram legend denote mean florescence intensity (MFI) of surface BST-2 levels. Experiments were repeated at least three times with similar results.

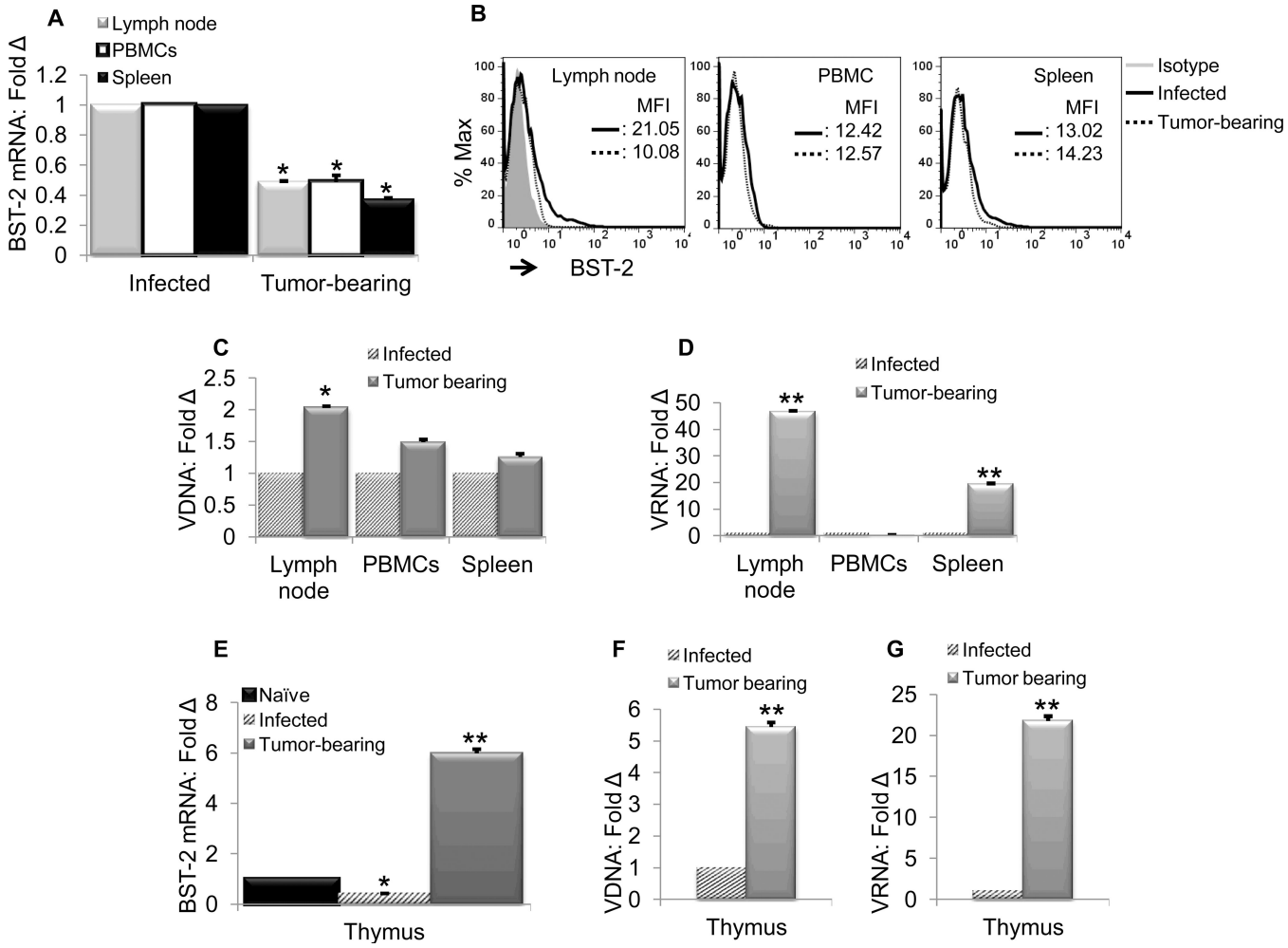

Figure 3. Differential BST-2 expression in murine lymphoid compartment during MMTV infection and carcinogenesis

C3H/HeN•MMTV+ mice infected via milk during nursing were sacrificed after 2 pregnancies (n = 5, age = 5 months) or allowed to develop mammary tumor (n = 5, age = 5 to 7 months). Mice bearing tumor were sacrificed in accordance to the policies of the University of Iowa Institutional Animal Care and Use Committee. Lymph nodes, PBMCs, and spleens as indicated in the figures were used for RNA and DNA extraction. RNA was used for determination of BST-2 mRNA by RT-qPCR (A). Single cells from these tissues were subjected to FACS analysis for BST-2 surface protein (B). DNA and cDNA were used for qPCR detection of viral DNA (C) while cDNA was used for viral RNA detection (D). Thymi tissues obtained from naïve C3H/HeN mice and the C3H/HeN•MMTV+ and their tumor-bearing counterparts described above were subjected to RT-qPCR to determine level of BST-2 transcripts and viral RNA (E and G). Thymic viral DNA was quantified using isolated DNA (F). RT-PCR data are normalized to GAPDH and presented as fold change relative to BST-2 mRNA or viral RNA in infected or naïve mice depending on experiment. Error bars are standard deviation; ** is significance with p value less than 0.01 and * is significance with p value less than 0.05. The numbers next to the legend denote mean

florescence intensity (MFI) of surface BST-2 levels. These experiments were repeated at least three times with similar results.

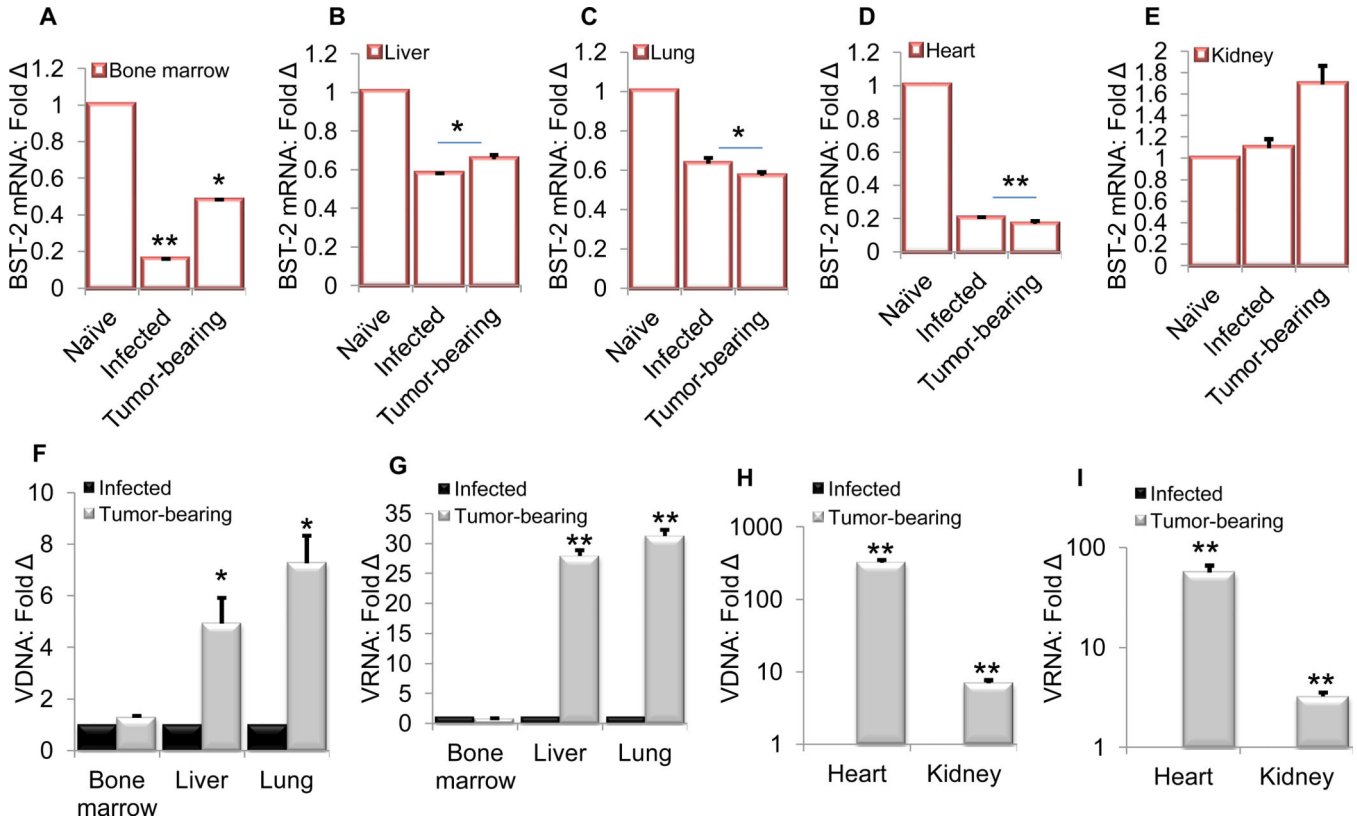

Figure 4. MMTV modulates BST-2 levels in non-lymphoid tissues

C3H/HeN•MMTV+ mice infected via milk during nursing were sacrificed after 2 pregnancies (n = 5, age = 5 months) or allowed to develop mammary tumor (n = 5, age = 5 to 7 months). As stated above, mice bearing tumor were sacrificed in accordance to the policies of the University of Iowa Institutional Animal Care and Use Committee. Following euthanasia, bone marrow cells, liver, lung, heart, and kidney were collected and used for DNA and RNA extraction. Reverse transcribed RNA was used to quantify BST-2 mRNA levels (A to E) and viral RNA levels (G and I). DNA was used to quantify proviral DNA expression (F and H). PCR data are normalized to GAPDH and presented as fold change relative to samples from the naïve and infected mice. Error bars are standard deviation; ** is significance with p value less than 0.01 and * is significance with p value less than 0.05. Experiments were repeated several times with similar results.

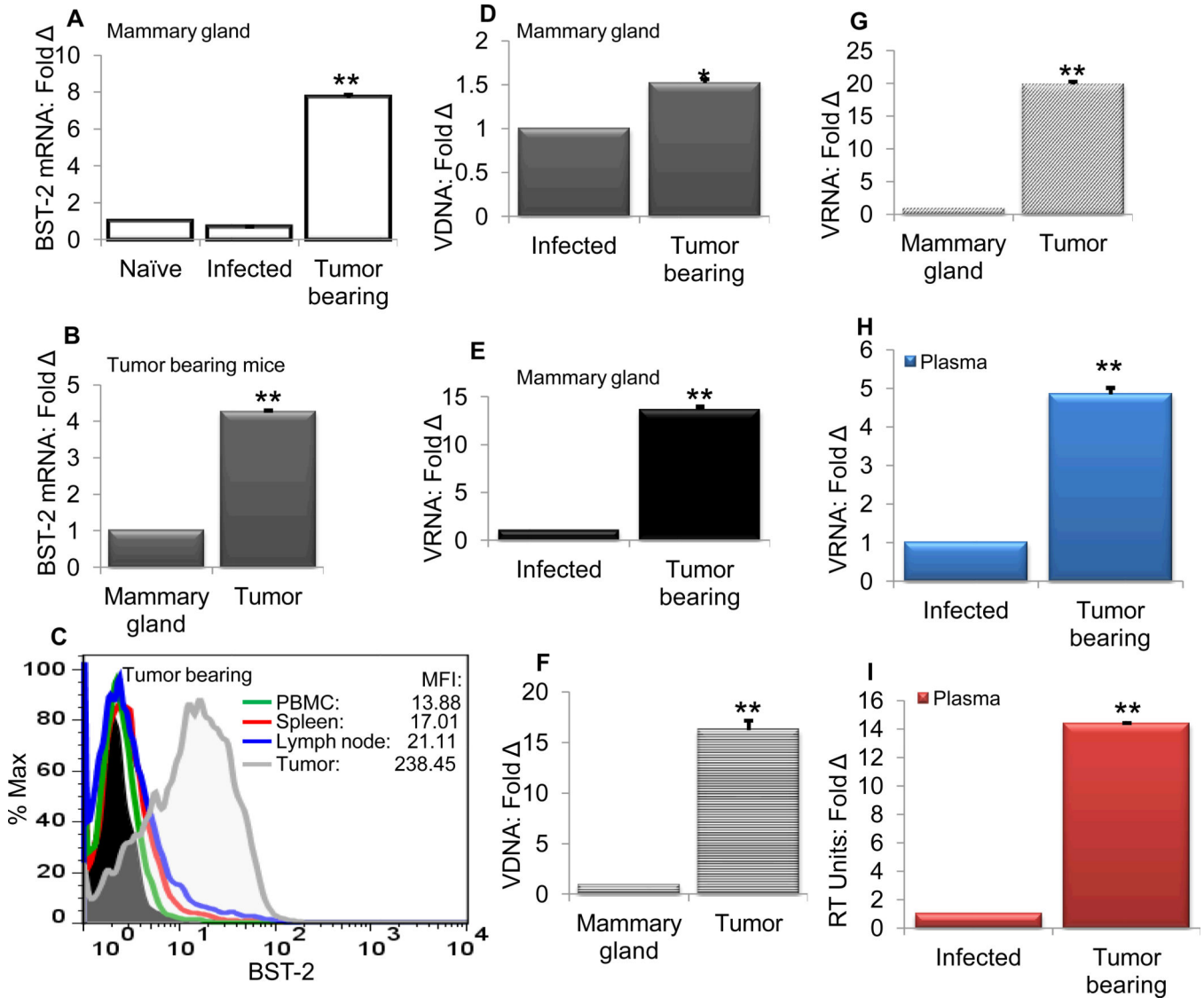

Figure 5. Mammary gland and Tumor tissues from C3H/HeN•MMTV+ tumor-bearing mice show high levels of BST-2 and viral nucleic acids

C3H/HeN•MMTV+ mice infected via milk during nursing were sacrificed after 2 pregnancies (n = 5, age = 5 months) or allowed to develop mammary tumor (n = 5, age = 5 to 7 months). As stated above, mice bearing tumor were sacrificed in accordance to the policies of the University of Iowa Institutional Animal Care and Use Committee. Mice were bled for PBMC isolation prior to euthanasia. PBMCs, lymph nodes, spleens, tumor tissues, and mammary gland tissues devoid of lymph nodes were used for DNA and RNA extraction. RNA was reverse transcribed to cDNA and used to quantify BST-2 mRNA levels (A and B). Single cells from the lymphoid and tumor tissues were subjected to FACS examination of BST-2 surface protein (C), while DNA was used to quantify proviral DNA (D and F); cDNA was quantified by RT-qPCR to determine levels of viral RNA expression (E and G). Cell-free plasma collected from the above infected and tumor-bearing mice (n = 5) were used for examination of plasma viral load by vRNA (H) or RT activity (I). All PCR data are normalized to GAPDH and presented as fold change relative to samples from the

naïve and infected mice. RT activity was extrapolated from the RT standard curve and presented as fold change of RT units in 1 μl of infected plasma. Error bars are standard deviation; ** is significance with p value less than 0.01 and * is significance with p value less than 0.05. The numbers next to histogram legend denote mean florescence intensity (MFI) of surface BST-2 levels. Experiments were repeated several times with similar results.

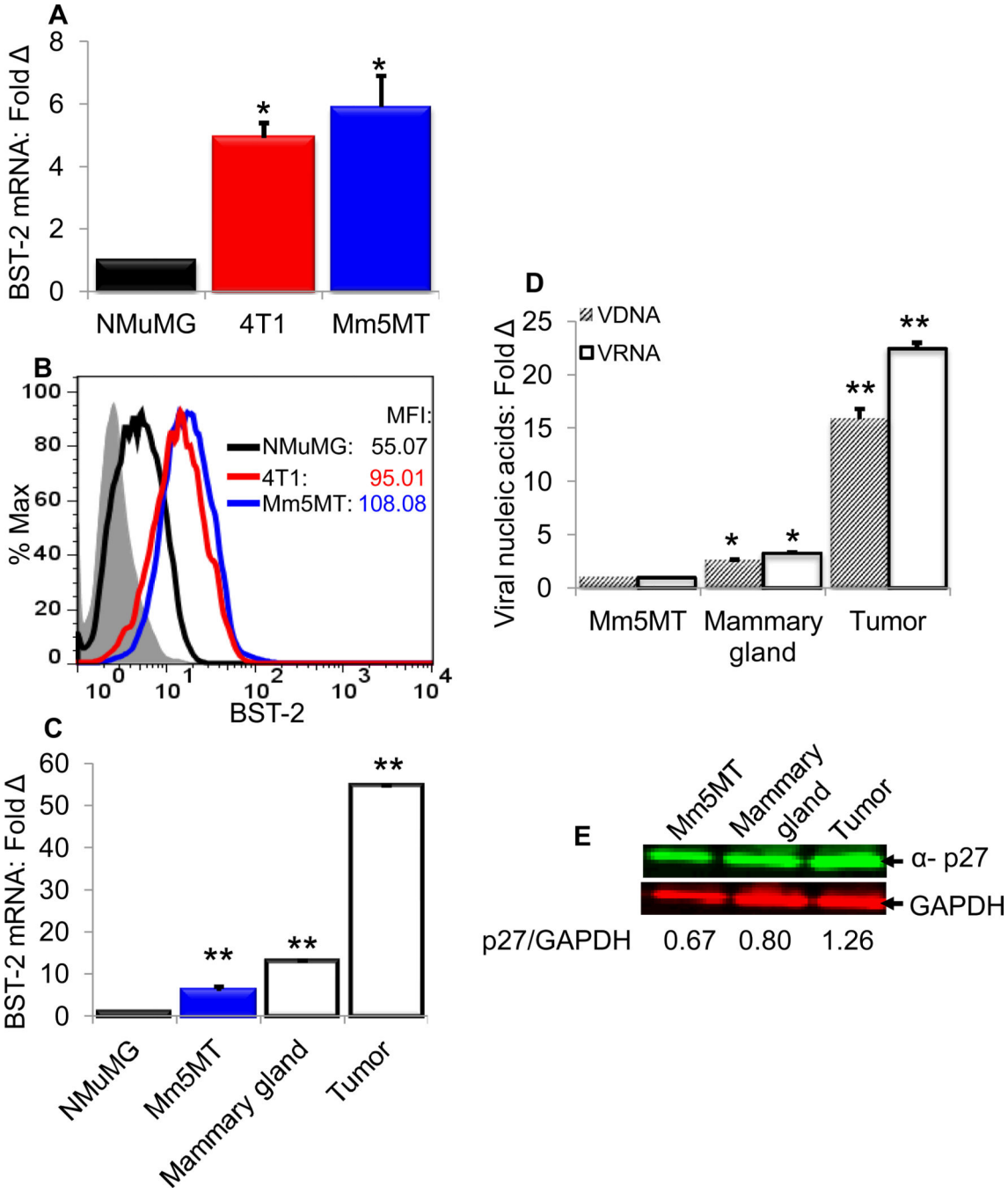

Figure 6. Mammary carcinoma epithelial cells overexpress BST-2 and viral nuclei acids

Normal mammary epithelial cells (NMuMG) and carcinoma mammary epithelial cells (4T1 and Mm5MT) were used for RNA extraction and RT-qPCR examination of BST-2 mRNA (A). A portion of cells were used for FACS analysis of BST-2 surface protein (B). RNA isolated from mammary epithelial cells (NMuMG and Mm5MT), mammary gland from tumor-bearing mice (n = 5) and mammary tumor tissues from the same mice were reverse transcribed and used to examine BST-2 transcripts by RT-qPCR (C). DNA, RNA, and protein isolated from cells and tissues as indicated in the figure were examined for levels of

proviral DNA and viral RNA (D) as well as viral protein (E). RT-qPCR and qPCR data are normalized to GAPDH and presented as fold change relative to samples from NMuMG or Mm5MT. Viral protein was detected with MMTV capsid antibody (α- p27) and GAPDH was used as loading control. Error bars are standard deviation; ** is significance with p value less than 0.01 and * is significance with p value less than 0.05. The numbers next to histogram legend denote mean florescence intensity (MFI) of surface BST-2 levels. All experiments were repeated 3 times with similar results.

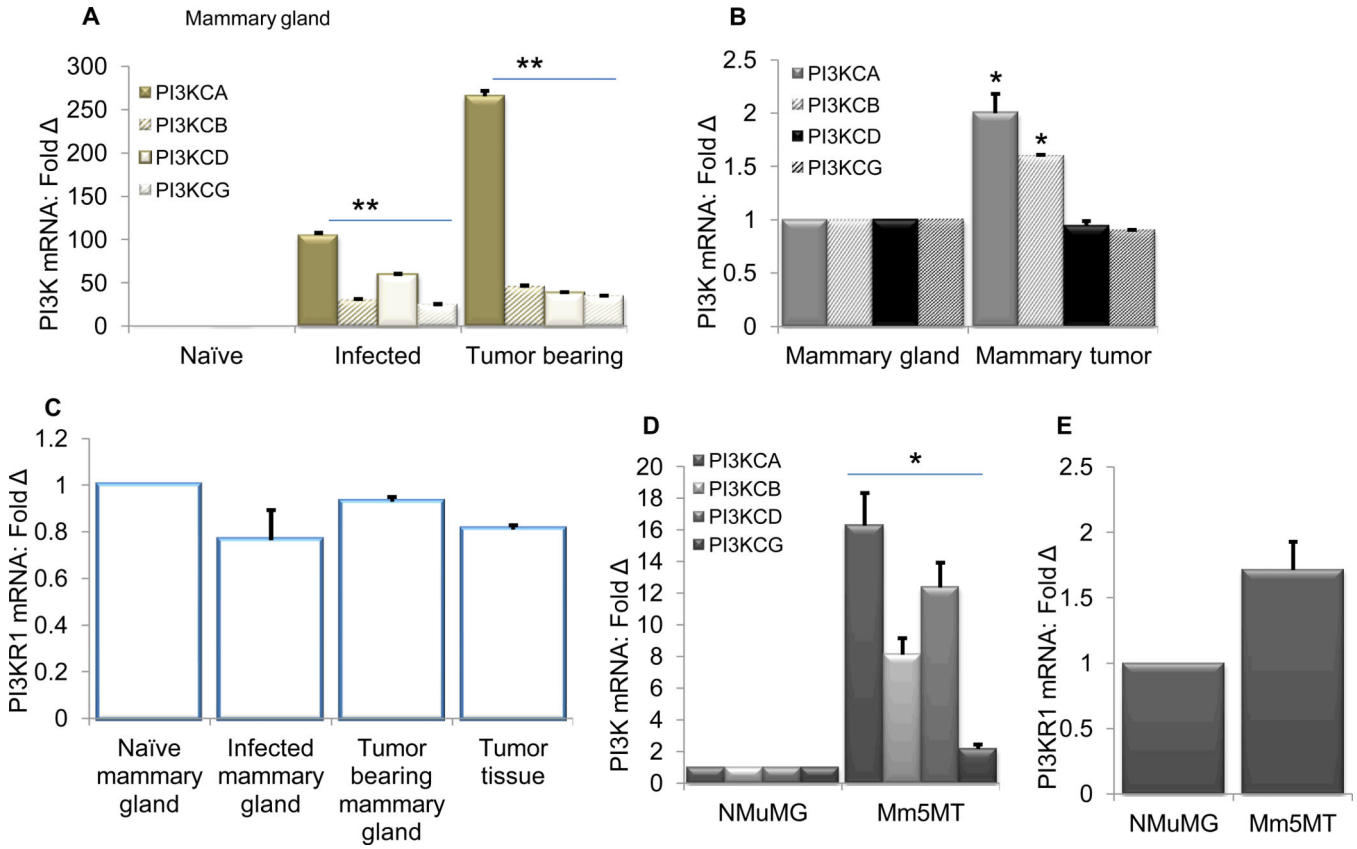

Figure 7. Expression levels of some PI3K isoforms in C3H/HeN mammary gland and tumor tissues positively correlate with BST-2

RNA isolated from mammary gland and tumor tissues from Naïve mice (n = 5), infected mice (n = 5), and tumor-bearing mice (n = 5) described in figure 5, or mammary epithelial cells (NMuMG and Mm5MT) described in figure 6 was used. Transcript levels of PI3KCA, PI3KCB, PI3KCD, and PI3KCG in mammary gland tissues (A) and mammary gland and tumor tissues (B) were compared by RT-qPCR analysis. Level of PI3KR1 mRNA was compared between mammary gland tissues and tumor tissue (C). PI3KCA, PI3KCB, PI3KCD, PI3KCG, and PI3KR1 mRNAs in mammary epithelial cells were analyzed by RT-qPCR (D and E). Graphs represent means and error bars are standard deviation; ** is significance with p value less than 0.01 and * is significance with p value less than 0.05. Experiments were repeated 3 separate times with similar results.

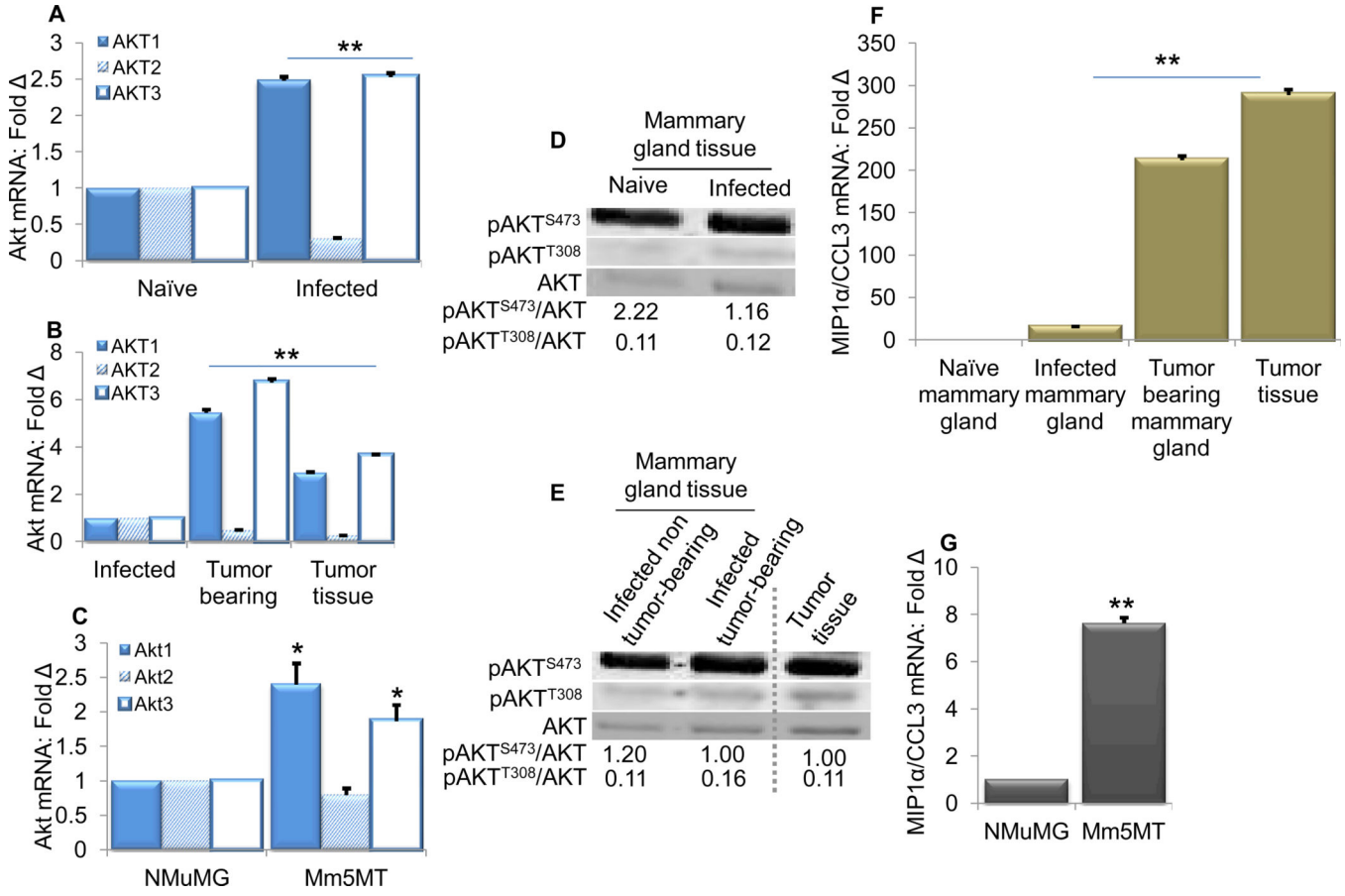

Figure 8. AKT1, AKT3, and MIP1α/CCL3 mRNA correlate with BST-2 but AKT2 mRNA does not correlate with BST-2 in mammary gland and tumor tissues of C3H/HeN

Transcript levels of AKT1, AKT2, and AKT3 in mammary gland, tumor tissues and mammary epithelial cells were determined by RT-qPCR analysis of cDNA obtained from total RNA of naïve mice (n = 5), infected mice (n = 5), mice bearing mammary tumor (n = 5), NMuMG, and Mm5MT cells (A to C). AKT protein level was determined by Western blot using total cell lysate probed with phospho-specific antibodies and total AKT antibody for loading control (D and E). Expression level of MIP1α/CCL3 in mammary gland, tumor tissues and mammary epithelial cells were determined by RT-qPCR analysis of cDNA obtained from total RNA of naïve (n = 5), infected (n = 5), mice bearing mammary tumor (n = 5), NMuMG, and Mm5MT cells (F and G). Graphs represent means and error bars are standard deviation; ** is significance with p value less than 0.01 and * is significance with p value less than 0.05. Experiments were repeated 3 separate times with similar results.

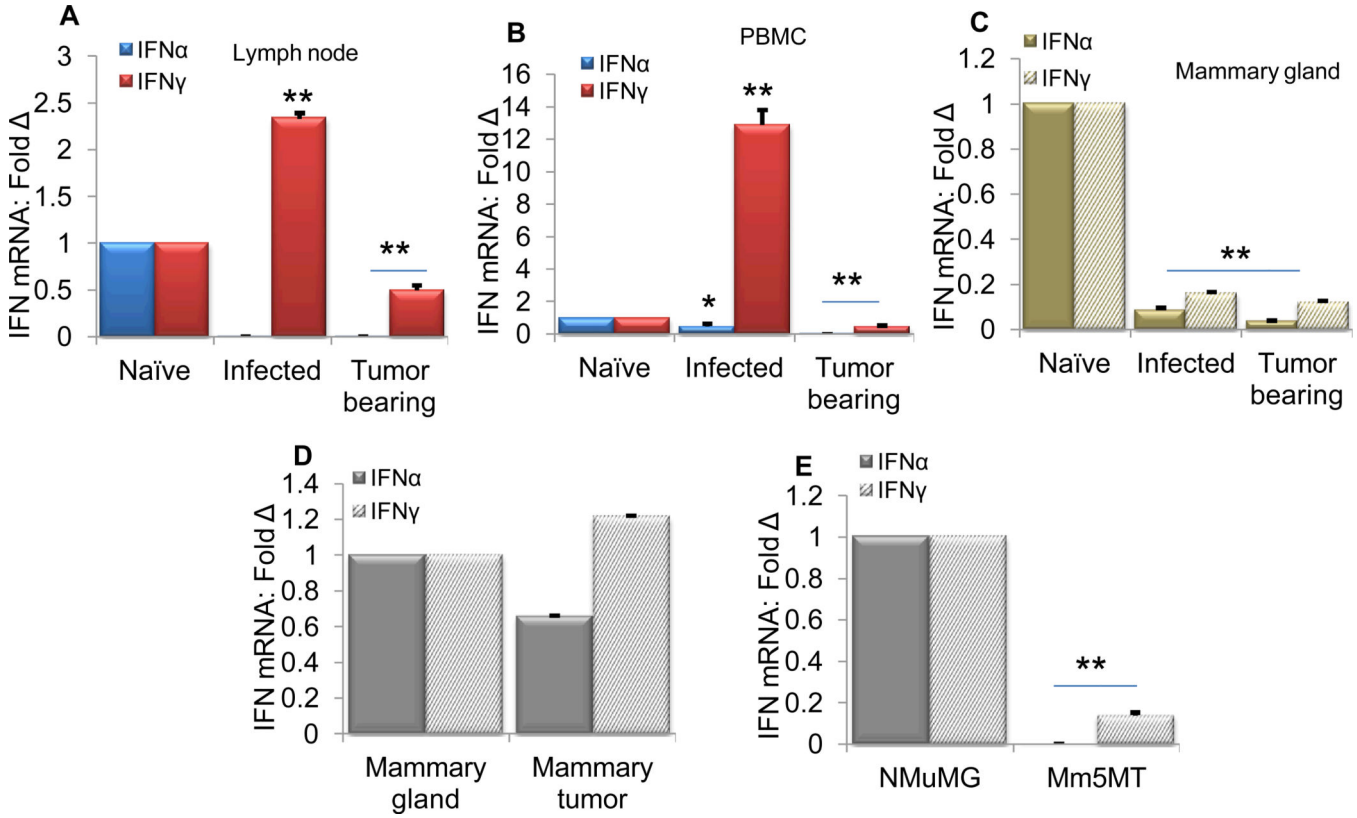

Figure 9. Levels of IFNα and IFNγ negatively correlate with BST-2 in tissues of mice bearing mammary tumor

Levels of IFNα and IFNγ in lymph node (A), PBMC (B), and mammary gland tissues (C) were analyzed by RT-qPCR of cDNA obtained from total RNA of naïve mice (n = 5), infected mice (n = 5), and mice bearing mammary tumor (n = 5). IFNα and IFNγ levels were compared between mammary gland and tumor tissues from the same mice (D), or between NMuMG and Mm5MT cells (E). Graphs represent means and error bars are standard deviation; ** is significance with p value less than 0.01 and * is significance with p value less than 0.05. Experiments were repeated 3 separate times with similar results.

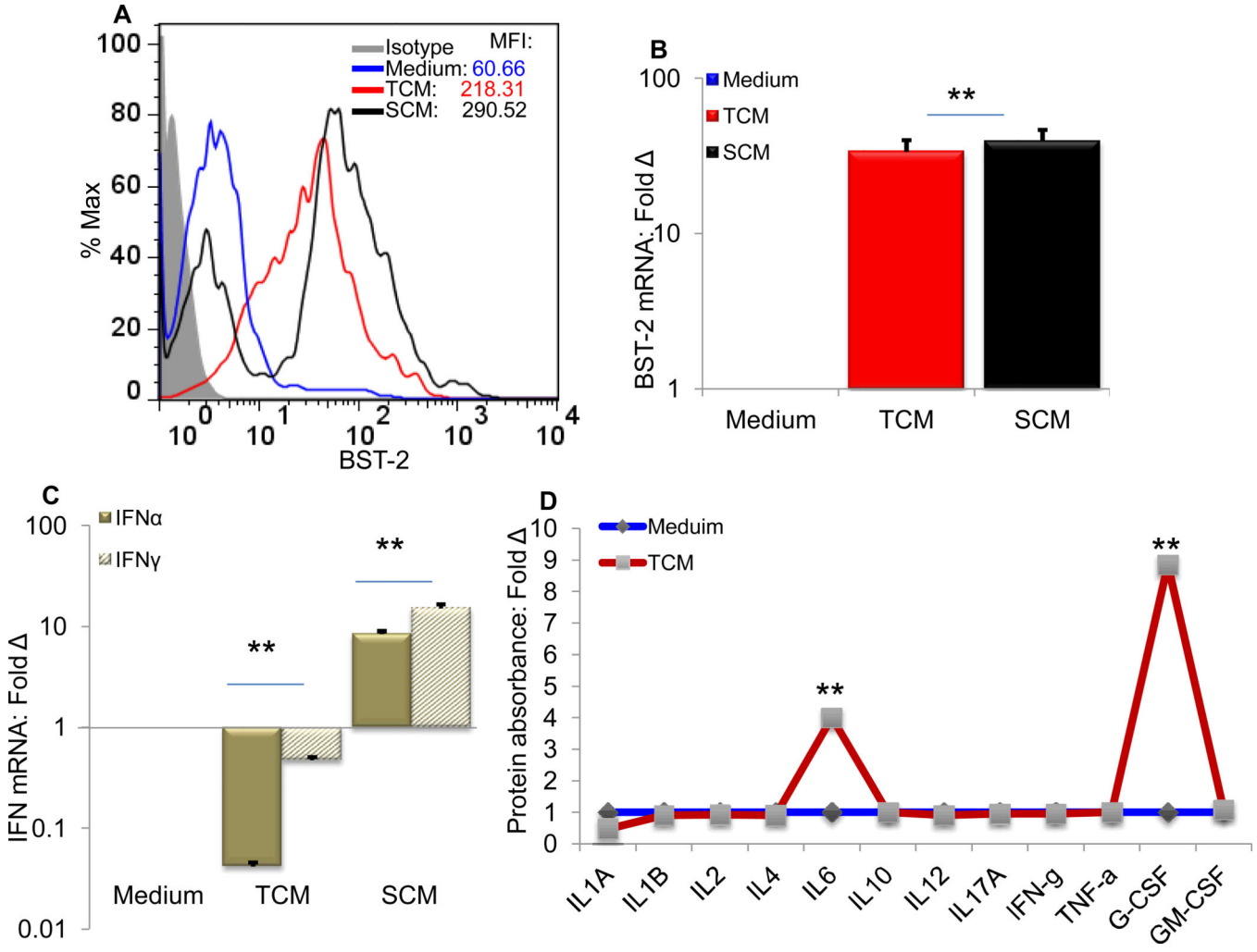

Figure 10. Tumor-conditioned medium mediates induction of BST-2 in mammary epithelial cells

Normal mammary epithelial cells (NMuMG) were cultured in normal medium (Medium), tumor conditioned medium (TCM), and splenocyte conditioned medium (SCM). A portion of cells were used for FACS analysis of BST-2 surface expression levels (A). The remaining portion of cells was used to determine level of BST-2 mRNA (B) and IFNα/IFNγ mRNA (C). Cell culture medium (Medium) and TCM devoid of particulate materials were used in mouse inflammatory cytokines multi-analyte ELISA to determine cytokines and/or chemokines present in TCM (D). Graphs represent means and error bars are standard deviation; ** is significance with p value less than 0.01 and * is significance with p value less than 0.05. The numbers next to histogram legend denote mean florescence intensity (MFI) of surface BST-2 levels. Experiments were repeated 3 separate times with similar results.